Hydrological Processes, Volume 28, Issue 8, pages 3241–3263, 15 April 2014
DOI:10.1002/hyp.9872

Hydrological modelling using data from monthly GCMs in a regional catchment

Renji Remesan [1], Tim Bellerby[2], Lynne Frostick[3]

[1] Centre for Adaptive Science, University of Hull, Now at: Cranfield Water Science Institute, University of Cranfield

[2]Department of Geography, Environment and Earth Science, University of Hull

[3]Centre for Adaptive Science, University of Hull

Abstract

This study demonstrates the use of spatially downscaled, monthly General Circulation Model (GCM) rainfall and temperature data to drive the established HyMOD hydrological model to evaluate the prospective effects of climate change on the fluvial runoff of the River Derwent basin in the UK. The evaluation results of this monthly hydrological model using readily available, monthly GCM data are consistent with studies on nearby catchments employing high-temporal resolution data, indicating that useful hydro-climatic planning studies may be possible using standard datasets and modest computational resources. HyMOD was calibrated against 5km^2 gridded UKCP09 data and then driven using monthly spatially-interpolated (~5km^2) outputs from HadCM3 and CCCMA for IPCC SRES A2a and B2a covering the 2020s, 2050s and 2080s. Results for both GCMs project a decrease in annual runoff in both GCM models and scenarios with higher values in the summer/autumn months; whereas an increase in the later winter months. Both HadCM3 and CCCMA show higher ranges of uncertainty during the winter season with higher values of runoff associated with December in all three simulation periods and two scenarios. A seasonal comparison of runoff simulations shows that both GCMs give similar results in summer and autumn whereas disparities due to GCM uncertainties are more conspicuous in winter and spring. In this study, both the GCMs under A2a scenario have demonstrated the high possibility of time

shift in monthly average peak runoffs in the Derwent River by 2080s in comparison to early 21st century.

***Keywords*:** CCCMA, HadCM3, auxiliary - HyMOD, parameter estimation, Blaney-Criddle potential evaporation, A2a, B2a, United Kingdom

Corresponding authors Address:

Vincent Building, Cranfield University, College Road, Cranfield, Bedfordshire,

United Kingdom MK43 0AL

E: r.remesan@cranfield.ac.uk

T: +44 (0)1234 750111

Introduction

The results from Global Climate Model (GCM) projections and recent studies (Parker et al. 1992; Fowler et al. 2005a; Hulme et al. 2002) suggest that anthropogenic climate change will result in changes to regional temperatures and other climatic processes yielding corresponding changes in rainfall intensity, variability and spatial distribution. This could lead to changes in future runoff characteristics that will require a rigorous and significant planning response with respect to freshwater resource management in order to secure a climate resilient and resistant economy. One aspect of this potential problem is flood risk. Some studies shown that in England and Wales alone, flood risk affects nearly five million people, two million homes, 185,000 business properties worth over £215 billion and agricultural lands worth over £7 billion (Soetanto and Proverbs, 2004; Harman et al., 2002). Recently the Yorkshire and Humberside region of the Northern England has witnessed unprecedented and frequent flood events with correspondingly significant impacts on the economy and society of the region. The Executive Summary of the Office of Science and Technology Report into Future Flooding (Foresight, 2004) suggests that England should anticipate an increase in Annual River and coastal flooding damage of £1–20 billion by the 2080s.

Over the last decade, a number of studies have employed conceptual hydrological models to analyse climate change impacts on runoff and water resources in different regions of the United Kingdom. Pilling and Jones (1999, 2002) downscaled and interpolated GCM data to a 10 x 10 km grid over the whole of Great Britain and later employed a 17-parameter hydrological simulation model (HYSIM) to predict an increased seasonality of flows, with markedly drier summers in Upper Wye catchment. Fowler *et al.* (2008) used large multi-model ensembles to derive probabilistic estimates for future flows in the Eden catchment. They used the Shuffled Complex Evolution (SCEUA) global optimisation algorithm to

calibrate the 6- parameter ADM model. Kay *et al.* (2006a, b) performed simulation using a conceptual PDM rainfall-runoff model, for 15 catchments across Great Britain based on the ~25 km grid resolution HadRM3H Regional Climate Model (RCM). These studies showed decreased flood peaks for a number of the catchments in the south and east of England with a future increase in winter mean and extreme rainfall. Catchments in the north and west showed an increase in flood peaks of up to 50% for a 50-year return period. Reynard *et al*. (2001) have used HadCM2 ensembles to drive a semi-distributed rainfall-runoff model and find out that winter flows are generally increased in the Severn and Thames catchments; and the highest flows occurring in higher frequency that before. Cloke *et al.* (2010) used the CATCHMOD hydrological prediction tool with HadRM3 outputs to evaluate flows in the River Medway in Southeast England from 1960–2080, showing a persistent lowering of mean daily river flows for all months in the year.

Uncertainty quantification is an important aspect of hydrological climate impact studies. Cameron (2006) adopted a conceptual rainfall-runoff model, TOPMODEL within the Generalised Likelihood Uncertainty Estimation (GLUE) methodological framework to assess hydrological modelling uncertainty associated UKCIP02 climate change scenarios. Kay *et al.* (2009) considered a range of potential sources of uncertainty in the estimation of flood frequencies under climate change, including: GCM structure; downscaling from GCMs/RCMs; hydrological model structure and hydrological model parameters. Many hydrological climate impact studies employ some form of bias correction of RCM/GCM outputs using either a simple linear bias-factor or nonlinear transformations (Graham *et al.* 2007a; Fowler and Kilsby 2007). Berg *et al.* (2012) have applied different bias correction methods ranging from simple scaling and additive corrections to more advanced histogram equalisation (HE) corrections to high resolution (7 km) regional climate model (RCM) simulations. Teutschbeina and Seiberta (2012) have an overview of available bias correction

methods, which were then evaluated for five catchments in Sweden using monthly RCM data.

Hydrological climate change impact studies may employ a range of model and data temporal resolutions. Monthly resolutions are relatively coarse with respect to the time scales of many hydrometerological and hydrological processes but enjoy greater data availability, both in terms of observations and model outputs. Arnell (1992) and Xu and Halldin (1996) successfully applied monthly hydrological models to explore the impact of climatic change on water management issues. Most of the GCM outputs supplied by the various modelling centres define large spatial–scale changes in monthly climate, which can be directly used in monthly hydrological models as inputs. Though not directly useful for flood forecasting, hydrological models driven using monthly GCM driven hydrological models have been successfully employed to study the adaptive measures that may be made in response to future pressure on water resources management, agricultural irrigation and environmental quality due to shrunken river flow rates. Panagoulia and Dimou (1997a, b) examined the differences in predictions of two monthly water balance (MWB) hydrological models under both historical and alternative climate conditions. Other example studies employing local scale monthly rainfall-runoff models under varying temperature, precipitation and other climate variables may be found in Arnell (1992), Xu and Halldin (1997) and Xu and Singh (1998). Jiang et al. (2007) used six different monthly water balance models to investigate hydrological process responses to different climatic scenarios in a river basin in China using GCM outputs. A good review of suitability of monthly hydrological models on climate impact studies and other specific hydrological purposes can find in Xu and Singh (1998). Teutschbeina and Seiberta (2012) have used monthly RCMs for hydrological simulations and to check capabilities of bias correction methods through the variability in hydrographs.

There are a number of advantages in using monthly GCM data and hydrological models for hydrological climate change impact studies, including: i) GCM climate change scenarios are readily available and relatively reliable ii) bias-correction is straightforward to derive (with due consideration to the *caveats* mentioned above); iii) monthly water balance models require fewer parameters to explain hydrological phenomena; iv) they are more readily applicable to ungauged catchments. Monthly discharge simulations are frequently sufficient for long term water resources management, including the development of adaptation strategies and long term river basin management schemes at large catchment or regional scale.

This paper applies a conceptual monthly hydrological model to study possible variations in the hydrological regime of Upper River Derwent in the Yorkshire and Humberside region of Northern England. High resolution downscaled data from (2.5 arc min; ~ 5-km^2 grid size) two well-known GCMs - the UK based HadCM3 and the Canadian CCCMA - were obtained for the A2a and B2a scenarios and used to drive a conceptual monthly hydrological model (auxiliary-HyMOD). HyMOD was calibrated using the Shuffled Complex Evolution Metropolis Algorithm (SCEM-UA) and bias corrected using the event bias correction methodology. The study focussed on model predicted annual and seasonal variations of runoff in the River Derwent catchment for standard projected periods covering the 2020s, 2050s, and 2080s

2. Materials and Methods

2.1 Study Area

The river Derwent is a major river in Yorkshire, Northern England with key influence on the local economy. Water abstracted from the Derwent supplies a number of large communities (such as Hull, Leeds, York and Scarborough) as well as agricultural holdings along its course. The river Derwent catchment is one of the eight major catchments within the Yorkshire-Humberside region, alongside the Aire, Don, Esk (and coastal streams), Hull (and coastal

streams), Ouse, Ribble and Tees. The catchment area covers approximately 1586km², draining to Buttercrambe (UK Ordnance Survey Grid Reference SE 731587) in North Yorkshire (Figure 1). At the source and upper regions, the major river and its tributaries run over Corallian limestone formations. The annual average rainfall in the region is 779 mm, out of which approximately 59% is accounted for as evapotranspiration. Annual rainfall over the northern half of the catchment (North York Moor) exceeds 1,000 mm in some years (Hutchins, *et al.*, 2010). According to the UK Land Cover Map (LCM2000), the major land uses in the region are arable, grass, woodland and upland cover, with respective areal proportions of 42%, 27%, 15%, and 13. The remaining areas are urban and suburban (Fuller et al., 2002).

2.2 Hydrological Data

This study used daily flow data at Buttercrambe gauging station (operator- EA, number- 027041, maximum altitude- 454.0 mOD) in the Derwent catchment obtained from the UK National River Flow Archive at the Centre for Ecology and Hydrology, Wallingford. (http://www.ceh.ac.uk/data/nrfa/index.html) for the period 1st October 1973 to 31st December 2008. 30m ASTER Global Digital Elevation Map (ASTER GDEM: http://www.gdem.aster.ersdac.or.jp) data were used to delineating the catchment.

2.3 Climate Datasets

Raw monthly 5km gridded climate data from the UK Climate Projections dataset (UKCP09) were obtained from the UK Met Office (http://www. metoffice.gov.uk/climatechange/science/monitoring/ukcp09/). Data including mean daily maximum temperature, mean daily minimum temperature, mean air temperature and mean precipitation were available for a period covering 1914-2006. To calculate the representative

values for the Derwent catchment, the gridded squares were averaged within a region running from 45°-50°E, 45°-50°N.

The major climate change scenarios reported by the Intergovernmental Panel on Climate Change Special Report on Emissions Scenarios (IPCC-SRES) (http://www.ipcc-data.org/) that describe "regionalization" are the A2a and B2a. The A2a scenario describes a highly heterogeneous future world with regionally oriented economies. The B2a scenario is also regionally oriented but with a general evolution towards environmental protection and social equity. In comparison to B2a, the A2a climate scenario assumes a higher rate of population growth, greater increases in GDP, the availability of less diverse and effective technologies, and wider changes in land-use (Leckebusch *et al*. 2004). This study used the standard monthly A2a scenario (widely coined "business as usual") outputs from two GCM models: the Hadley Centre Coupled Model, version 3 (HadCM3) and Canadian Centre for Climate Modelling and Analysis CCCMA) model covering the 2020s, 2050s, and 2080s. These data were employed at a monthly time step but had to be spatially downscaled.

A range of downscaling methods have been adopted to perform regional and local-scale impact studies. One of the simplest and most widely used downscaling approach is the use of "change factors" (CFs) (Arnell, 2003; Diaz-Nieto and Wilby, 2005) also known as so-called 'delta method' or 'perturbation method' (Prudhomme *et al*., 2002). A limitation of this approach is that it ignores the spatial variability of the climate and assumes that spatial patterns remain constant (Fowler, *et al*., 2007). Other statistical downscaling approaches include regression models weather typing schemes and weather generators (Abaurrea and Asın (2005); Bergant and Kajfez-Bogataj (2005); Enke *et al*., 2005; Fowler *et al*., 2005b). The use of regional climate models (RCMs) or limited-area models on the GCM outputs are generally referred as dynamic downscaling. Climate ensembles of multiple GCM- RCM driven simulations are available through projects such as PRUDENCE (European FP5

Prediction of Regional scenarios and Uncertainties for defining European Climate change risks and Effects), ENSEMBLES (EU FP6 project), NARCCAP (North American Regional Climate Change Assessment Program) (Christensen et al., 2007; Mearns et al., 2006), *WorldClim* (Hijmans *et al*., 2005) and the International Centre for Tropical Agriculture (CIAT) GCM portal. The Statistical and Regional dynamical Downscaling of Extremes for European Regions (STARDEX) project compares available statistical, dynamical and statistical–dynamical downscaling procedures (Fowler *et al*., 2007).

As noted above, this study aims to demonstrate the utility of readily available monthly data for hydrological modelling, including a basic assessment of changes to flood risk. Monthly precipitation fields are generally smoother than the daily, easing the spatial downscaling problem to some degree. In keeping with the aim of generating impact assessments using readily available datasets, the study has focused on the globally available high-resolution *WorldClim* dataset (Hijmans *et al*., 2005). The projected high resolution GCM data of 2.5 arc min (~ 5-km^2 grid size) was obtained from the WorldClim database and CIAT GCM downscaled data portal. These data are downscaled using a variant of the Delta Method approach, in which GCM predicted anomalies are interpolated to a higher resolution. This Delta method is based on thin plate spline spatial interpolation of anomalies (deltas) of original GCM outputs; and this method is performed on two assumptions that 1) climatic changes are only relevant at coarse scales and 2) that relationships between variables are maintained towards the future. The delta method has following steps (Ramirez and Jarvis., 2010) 1. Gathering of baseline data and full GCM time series, 2. Calculation of running averages for present and future climate, 3. Calculation of anomalies as the absolute difference between future values in each of the variables (precipitation, maximum and minimum temperature) to be interpolated, 4. Interpolation of these anomalies using centroids of GCM cells as points for interpolation, 5. Addition of the interpolated surfaces to the current

climates from WorldClim, using absolute sum for temperatures, and addition of relative changes for precipitation, 6. Calculation of mean temperature as the average of maximum and minimum temperatures. The detailed mathematical formulation of this method is given in Ramirez and Jarvis (2010). This interpolation procedure yields arc-second surface of changes in climates for each of the variables for the selected months. These surfaces are then applied to the baseline climates from WorldClim. All these calculations can be done by using any automatable GIS software.

Five kilometre GCM outputs for the Derwent catchment show high spatial variability in both Temperature and Precipitation. A simple systematic technique was adopted to estimate the corresponding hydrological uncertainties. Systematic input combinations were constructed using different collections of the maximum, minimum, and mean values of GCM derived monthly variables spatially distributed in the catchment. 27-different input space were generated for each GCM by adopting different combinations for each of the three projected decades of the maximum, minimum and mean values of monthly precipitation with corresponding values from spatial Blaney-Criddle based potential evaporation series tabulated from GCM-derived monthly maximum, minimum or mean daily temperatures. The underlying assumption in adopting these systematic ensembles of inputs is that that these values are equally likely to occur as catchment average at one point of time in each time slices, and that the these ensembles includes the full range of extremes that are likely to occur in the catchment. This basic input selection is not sufficient to quantify uncertainty probabilities but should provide a meaningful spread of variability (innate in the system or cascaded) and encompass variations in the regional effects of rainfall patterns.

2.4 The Hydrological Model, HyMOD

The five-parameter Hydrological MODel (HyMOD) was originally proposed by Boyle (2001) based on the general concept in article by Moore (1985) describing an extension of the Probability Distributed Moisture (PDM) lumped storage model. The HyMOD concept consists of a simple, probabilistic, rainfall excess representation connected to two series of linear reservoirs (three identical reservoirs for quick flow response and a single reservoir for the slow flow, groundwater response). Each point in the catchment is assumed to have a capacity (C) of which a portion is filled up as water storage. When the water storage capacity is exceeded, excess of water drains out the catchment as runoff. The model further assumes a distribution function for this varying water storage capacity of the catchment as follows:

$$F(C) == 1 - \left(1 - \frac{C}{C_{max}}\right)^{b_{exp}} \qquad 0 \leq C \leq C_{max} \tag{1}$$

Where, F(C) is the cumulative probability of a given water storage capacity C. The five model parameters are C_{max}, b_{exp}, Alpha, R_q and R_s, respectively representing the maximum storage capacity within the watershed, the degree of spatial variability of the soil moisture capacity within the watershed, a factor partitioning the flow between the two series of linear reservoir tanks, the residence time parameters of quick-flow tanks and the residence time parameters of slow-flow tanks respectively. These parameters must be optimized with respect to observed stream flow data. The model has been widely applied in scientific evaluation of new concepts in hydrology (Wagener et al., 2001; Moradkhani et al., 2005; Vrugt et al., 2003a, 2003b).

The model uses two input variables: mean precipitation (*P*) and potential evapotranspiration (*ETp*). In this study, potential evapotranspiration data were generated as per Fowler and Kilsby (2007) using the well-known Blaney-Criddle approach (Blaney and Criddle, 1950):

$$ET_p = p_t(\alpha T + \beta) \tag{2}$$

Where p_t is the mean daily percentage of annual daytime hours T is mean temperature in °C. A and β are empirical constants. Walsh and Kilsby (2007) have identified these values as 0.456 and 0.416 respectively. The p_t value corresponding to approximate latitude of the location could be determined from the FAO irrigation water management training manual (Brower and Heibloem, 1986).

The HyMOD generally operates at a daily time step. Winsemius *et al*. (2009) adopted an auxiliary rainfall-runoff model (auxiliary HyMOD) working on monthly timescale data, following ideas in Seibert (2001) and Schaefli and Gupta (2007). The auxiliary HyMOD was calibrated at a monthly timescale to reproduce estimates of mean monthly discharge for any period for which monthly rainfall was available, without altering the structure of the model. If a conceptual model is applied in monthly time steps the storage of the direct runoff tank should not held back at all or longer. Similarly this study has adopted a monthly time step 5-parameter auxiliary-HyMOD and compared the results with traditional daily HyMOD model. Another monthly water balance model adopted by Winsemius et al (2006) is a Lumped Elementary Watershed (LEW), which follows the principles of HyMOD with two slow tanks and one quick tank. In this study, the parameters for the auxiliary - HyMOD were determined using the University of Arizona implementation of the shuffled complex evolution Metropolis algorithm (SCEM-UA; Duan et al., 1992).

2.5 Shuffled Complex Evolution Metropolis Algorithm (SCEM-UA)

The Shuffled Complex Evolution Metropolis algorithm (SCEM-UA) was used to optimize abovementioned parameters as this approach is well suited to infer the posterior distribution of hydrologic model parameters. One advantage of the SCEM-UA approach is that operation of it combines the strengths of the Markov Chain Monte Carlo (MCMC) based Metropolis algorithm (Metropolis et al., 1953), controlled random search (Price, 1987), competitive evolution (Holland, 1975), and complex shuffling (Duan et al., 1992). The SCEM–UA

concept was developed by Vrugt et al. (2003b) at University of Arizona based on the Shuffled Complex Evolutionary (SCE–UA) (Duan et al., 1992) and it uses Bayesian inference scheme to identify the best parameters alongside its posterior distribution. Details of these algorithms can be found in Vrugt et al (2003b) and Duan et al (1992).

2.6 Bias-correction

In order to effectively employ the model outputs for water resources or flood frequency forecasting, some account must be made of systematic biases within the combined modelling system. There are several ways of dealing with model biases in runoff prediction and forecasting, including. distribution-oriented verification approaches (Murphy and Winkler, 1987), event-bias correction methods (Smith et al.,1992; Hashino et al., 2006), regression methods (Cleveland, 1979) and quantile mapping methods (Leung et al. ,1999; Wood et al., 2002). This study employed an event bias correction method and evaluated the runoff prediction with and without bias correction. The bias corrected stream flow z_j^i is given by

$$\boldsymbol{z_j^i = b_j^i . \overline{y}_j^i} \quad (3)$$

Where b_j^i is the multiplicative bias associated with the weather sequence for month *j* and year *i* and which can be calculated from the following equation in which Smith et al. (1992) estimate the multiplicative bias with observed and simulated flows from the historical record as:

$$\boldsymbol{b_j^i = \frac{y_j^i}{\tilde{y}_j^i}} \quad (4)$$

Where y_j^i is the observed stream flow for month *j* in year *i and* $\tilde{y}_j^i$ is the model-simulated stream flow for month *j* in year *i* from the historical data

Results and Discussions

3.1 Variability of Temperature and Precipitation Trends in the Study Region

Temperature and Precipitation trends in Derwent catchment during the 20th century (from year 1914) were analysed using recently updated and adjusted UK Climate Projections (UKCP09) historical data set. The projected trends were analysed using HadCM3 and CCCMA model outputs for various A2a and B2a scenarios. These details are shown in the Figure 2 and Figure 3 and their salient features are discussed in following subsections.

Historical Trends

After analysing 1914-2006 meteorological data, anyone can effortlessly find that there is distinct pattern of change of temperature in the Derwent catchment area for different seasons. This pattern is mostly evident in winter and summer with distinct drop in temperature during 1960-1969. The decadal changes of average precipitation and average temperature in comparison to corresponding values of antecedent decades are shown in the Table 1. In the case of historical winter and summer temperature, there is a statistically significant positive trend in the Derwent catchment from 1960-1969, which accounts for a value of 1.6^{0}C and 1.4 ^{0}C respectively. The trends in decadal mean temperature are depicted in Figure. 2 for 1914–2006 periods. One can note that there is rise of temperature prior to the 1940-1949s and after that there is a modest decrease up to 1970–1979 during autumn and spring seasons. The spatial pattern of temperature is also highly variable in the catchment from season to season. Among the four seasons, spring and autumn showed the greatest warming in early 21st century in comparison to 1914-1919 periods. The increase in average warming during 1914–2006 period is 0.89 ^{0}C, 1.12 ^{0}C, 1.29 ^{0}C and 1.79 ^{0}C respectively during winter, spring, summer and autumn.

In the case of average precipitation, no distinct trend has observed in the catchment during 1914-2006 for different seasons. The decadal variations of precipitation are shown in the Table 1. Across the catchment, precipitation has increased by 25% to 31% in different seasons except winter season during 2000-2006 periods in comparison to previous decade. The high variability of precipitations in different decades can be identified from the Table 1, with several positive and negative decadal trends. The percentage increase in winter precipitation was greatest during 1990-1999 periods, whereas the negative trends were observed in the case of other three seasons during same decade. The Figure 3(d) shows that there is 17.5% decrease in rainfall from 1914-1920 (78.28mm/month) to 2000-2006 period (64.56mm/month). During last century the lowest winter monthly rainfall rate was observed during 1980-1989 (57.93 mm/month) and now it has increased by 11.4% from that period.

3.1.2 GCM Outputs

The Seasonal changes in mean temperature; mean precipitation and mean PET (using Blaney-Criddle Formula) were calculated for three future time periods and pictorially compared to corresponding observed values for 2000-2006. A pictorial representation of predicted seasonal variations in mean temperature predicted as per CCCMA-A2a, CCCMA-B2a, HadCM3-A2a and HadCM3-B2a are shown in Figure 2, along with historical trend from the year 1914. Seasonal GCM simulation precipitation outputs from the CCCMA and HadCM3 based on the Special Report on Emissions Scenarios (SRES) A2a and B2a scenario for the Derwent river catchment are shown in the Figure 3, along with historical decadal trends from year 1914. The percentage variation of projected meteorological variables in comparison with early years of 21st century is also given in the Table 2. The sub sections below present the characteristics of variations of climate variables predicted by GCMS in different seasons in comparison to observed values.

3.1.2.1 Winter and Spring

The study has compared the downscaled GCM data outputs (finer scale of 5 Km^2) with the UKCP09 historical data sets for the different seasons (Table 2). The projected winter precipitation data obtained from the two GCMs shows reasonably high variability throughout the study region for both scenarios in winter and spring seasons. All seasonal temperature values observed during A2a scenario have shown relatively higher warming in projected periods in comparison to B2a scenario for both models with slight disparity in CCCMA model during 2020s winter season. As the PET was estimated using Blaney-Criddle formula (the equation is a function of temperature), the variation of projected PET values have followed comparatively similar trends like that of the temperature variation. The pictorial display of variation of PET within the catchment for different A2a seasons from both CCCMA and HadCM3 models are shown in the Figure 4 during 2020s, 2050s and 2080s. In winter season, the PET estimated using Blaney-Criddle formula and downscaled CCCMA-A2a derived climate variables has shown a change of 1.91%, 20.59%, and 31.35% for the study instances like 2020, 2050 and 2080 respectively in comparison to the 1999-2008 average. The HadCM3-A2a derived PET values have shown a change of -6.16%, 17.70%, and 38.59% respectively. In B2a scenario, a decrease in winter PET observed in HadCM3 2020s simulations with value of -6.17% (as simulated 2020s mean temperature in the catchment area is slightly smaller than the baseline temperature (-0.049°C)). An increase in PET are 17.70% and 38.59% respectively for the HadCM3-B2a simulations for the time slices 2050s and 2080s, while the values corresponding for the CCCMA-B2a simulations are 0.08%, 7.71% and 20.23% for study periods 2020s, 2050s and 2080s. The Figure 4 would also give an idea of the spatial variation of temperature within the catchment under different seasons. The general GCM results have shown that monthly averaged seasonal precipitation values are decreasing in the study area for all seasons except winter season, in comparison to

the average values of baseline period. Contradicting results have shown by two models in the case of B2a winter precipitation during 2020s and 2050s (Table 2). It is also interesting to note that HadCM3 model has predicted negative trend in winter precipitation and temperature during 2020s for both A2a and B2a scenarios with fairly highly positive trend during 2050s and 2080s. HadCM3 model in both A2a and B2a have shown positive trends in monthly averaged spring precipitation during 2080s whereas the CCCMA has produced negative percentage changes.

3.1.2.2 Summer and autumn

The main features of change for the summer months are the radical reduction in effective monthly precipitation over the entire study area and rapid change in the summer temperatures. One can observe a steady increase in summer precipitation reduction from 2020s to 2080s in all GCM models except the CCCMA model in A2a scenario. In the case of CCCMA-A2a model, the precipitation reduction value at 2080s is not high as that of 2050s. The mean seasonal temperature during summer may decrease in the 2020s in comparison to 2000-2006, for scenarios like CCCMA-A2a, HadCM3-A2a and HadCM3-B2a. One can find in the Table 2 that, the changes in monthly PET summer and autumn values are consistently increasing in both the scenarios and models from study period 2020s to 2080s in comparison to the 2000-2006 periods. There isn't any definite pattern in negative trend changes in autumn precipitations during 2020s to 2080s. A slight reduction in autumn temperatures are expected in the case of A2a scenario of both the models during 2020s; whereas positive changes are expected in the case both HadCM3-B2a and CCCMA-B2a models. The CCCMA-A2a derived summer PET percentage changes are -0.063%, 7.566% and 14.45% whereas the HadCM3 derived PET changes are -2.29%, 4.571% and 12.44% for the instants like 2020, 2050 and 2080 respectively in comparison to tabulated PET mean values corresponding to years 1999-2008. It is observed that the monthly summer PET changes are

consistently increasing in both the scenarios from study period 2020s to 2080s. Between the current baseline period and the 2080s, there are on average increases in monthly summer PET of about 8.28% under CCCMA-B2a scenario and about 7.70% under HadCM3-B2a scenario. There are an average increases in monthly summer PET of about 1.09% and 3.47% under CCCMA-B2a scenario whereas a change of -1.58% and 2.95% was observed under HadCM3-B2a scenario during 2020s and 2050s respectively.

3.2 Hydrological Modelling and Parameter Estimation

3.2.1 Modelling with Monthly Timescale auxiliary-HyMOD

The fluvial hydrology of the River Derwent catchment was assessed through use of a relatively simple rainfall excess model (an auxiliary-HyMOD) operating on monthly scale data obtained from GCMs in A2a and B2a scenarios. The five parameters of this monthly scale HyMOD conceptual model were determined using the SCEM-UA algorithm operating on monthly data obtained from the UK National River Flow Archive (Buttercrambe gauging station) and UKCP09 observed data corresponding to the Derwent catchment during the period of October 1973 to December 1999. The remaining six years of UKCP09 data was used for testing. The modelling system was initialized by defining the prior uncertainty range associated with the parameters. The details of the parameter bounds, their best behaviour range and expected values of parameters are shown in the Table 3.

The effectiveness of the SCEM-UA algorithm in parameter convergence was assessed through the transition of the Gelman and Rubin (GR) (Gelman and Rubin, 1992) scale-reduction convergence diagnostic for each of the model parameters. As per their recommendation, when the GR quantitative conversion diagnostic drops below 1.2, the convergence to a stationary posterior distribution can be assumed. The SCEM-UA algorithm effectively determined the parameter space, with convergence to a stationary posterior distribution (GR diagnostic < 1.2) for all five parameters at around 4900 simulations. Figures

5(a) to 5(e) present the frequency histograms for each of the auxiliary – HyMOD model parameters obtained from the River Derwent catchment data through the SCEM-UA algorithm. Figure 5(f) shows the evolution of the GR scale-reduction convergence diagnostic for each of the model parameters. Figure 6 illustrates the performance of these estimated parameters at predicting runoff. This figure also shows the ±95% confidence interval of the uncertainty ranges.

3.2.2 Bias Correction and Comparison of Modelled Results

In the Figure 6, one can note that the auxiliary-HyMOD, fails to simulate higher discharge values for some years in the simulation period. The monthly timescale auxiliary - HyMOD performed better during drier months of the simulation period but with underestimations in larger peaks of certain years. Though, the estimated parameters of the auxiliary HyMOD performed well in mimicking the runoff pattern, there was a notable bias in the simulation results. As the aim of the study is to use the capability of auxiliary - HyMOD in simulating future mean runoff, an event bias correction was applied to its simulation results. Table 4 shows the improvement in prediction after application of the event bias correction method.

In order to assess the robustness of the correction method employed, model performance was evaluated using a range of statistical indices including: bias, mean absolute error (MAE), mean square error (MSE), the root mean square error (RMSE), and the correlation coefficient (CORR) and Nash–Sutcliffe (NS) model efficiency (E). A summary of the performance of the HyMOD model before and after event bias correction is shown in Table 4. Higher values of Bias and RMSE during the winter months could be associated with difficulties in simulating snowfall related runoff. RMSE is also relatively high during the summer and later months of spring. For June and September, bias values are relatively small, but correlation values show that their linear association is relatively low. The second part of Table 4 shows how bias correction affects model performance. The NS model efficiency and linear

correlation values (CORR) were considerably improved after the bias correction especially in winter months. The NS efficiency has improved to a value higher than 0.8 in all months. Table 4 is also presented a statistical comparison of annual values, showing positive results after bias correction. The NS efficiency associated with the annual values have increased by 15.2 % after the bias correction. The coresponding changes in MSE and statistical bias can also find in the Table 4. The higher quantity of bias was observed in the annual data before the corection approach with value of -0.638 m3/s and this value could improved to -0.299 m3/s after the correction approach. The observed and estimated runoff values of auxilary-HYMOD model for the calibration data (1974-1999) given in Figure. 7 in form of a time series plot along with corresponting time series after bias correction. The coresponding values for the validation data (2000-2006) is given Figure 8 in the form of a time series plot. The statistical comparison of training and validation data sets are given in the Table 5.

To further understand the effect of modelling at a monthly time step and the associated bias correction, flood frequency curves corresponding to 33 years (includes training and validation data) observed flood data were ploted and compared with those of the HyMOD prected and bias corrected flow series (Figure 9). The monthly time-step auxilary - HyMOD simulations (without model bias correction) produce acceptable flood estimates up to a recurrence interval of 10 - 30 years and exhibits underestimation towards the 50-year return periods and higher. The disparity primarily corresponds to a single event. In October and November of year 2000 Yorkshire and Humberside experienced the worst flooding in 375 years. However the event bias correction method effectively tackles this problem giving a better fitting flood frequency curve (Figure 9).

3.3 Climate Change Impacts on Fluvial Hydrology

3.3.1 A2a Scenario

In this section, the impact of the expected climate change under the A2a scenario was examined by comparing stream flow simulated by driving the monthly time-step auxiliary - HyMOD using GCM data from CCCMA and HadCM3 monthly outputs for the 2020s, 2050s and 2080s with observed stream flow for recent 10 years (1999-2008). Uncertainty ranges for monthly flow regimes were calculated using the wettest and driest systematic ensemble input combinations for each month. The study has hydrological simulations using 27 distinct ensemble input combinations for each time slices (2020s, 2050s and 2080s) for both GCMs. The details of ensemble combinations are given in the table 6. Strictly speaking, though, this sort of systematic ensemble analysis is not fully representing all possible uncertainties associated with the modelling, the resulting hydrological variations produced by these different ensemble combinations can be considered as a measure of model sensitivity. Figure 10(a) shows the ensemble of auxiliary-HyMOD simulations obtained by using different input structure in the SRES CCCMA-A2a a scenario during the time slice of 2050s, the corresponding ensemble simulations results for SRES HadCM3-A2a can found in 10(b). Figure 11 shows the monthly percentage change in runoff between the future SRES A2a CCCMA simulations and observed values in 1999-2008 time slices at the river Derwent catchment, showing results for three periods (the 2020s, 2050s and 2080s). The uncertainty bounds at each case are provided as error bars, which have simulated from distinct ensemble combinations of inputs for the optimum parameter set suggested by SCEM-UA procedure.

Figure 11 shows that the larger uncertainty bound is associated with December (in all three periods (2020s, 2050s and 2080s) A lower range of uncertainty is observed during the summer and early months of autumn (July, August, September and October). The pattern of

uncertainty range is similar for all three predicted periods, with a slight increase in uncertainty from 2020s to 2080s. However in the autumn and early winter the uncertainty ranges tend to decrease from the 2020s to the 2080s. In general the SRES A2a CCCMA model based simulation shows definite stream flow reductions during summer and autumn (June to November). The simulation results suggest an increase in winter flow during February of 2050s and 2080s. The results also indicate that early winter (December) flood flows may increase during the 2050s. Percentage changes between the observed monthly stream flow for 1999-2008 and SRES A2a HadCM3 GCM model derived future scenarios are shown in the Figure 12.

SRES A2a HadCM3 simulations show the same trend in uncertainty ranges as the CCCMA model with higher ranges in winter season and lower ranges in summer/early autumn season. The late winter stream flow (February) shows a large increases. However, the HadCM3-based simulation exhibited a reduction in flow in early winter (December) Flood flows in early and later months of spring (March and May) are higher in the 2080s The HadCM3-based forecast shows clear-cut reductions in summer flows, autumn flow and early winter flows with higher numerical values than that of CCCMA models.

A comparison on average annual stream flow in a catchment for predicted future climatic conditions should give a strong indication of changes in resource availability. Both the CCCMA and HadCM3 models show a considerable reduction in annual runoff in the River Derwent catchment in comparison to stream flow during 1999-2008. During 1999-2008, the Yorkshire-Humberside region has experienced high rainfall variability increased rainfall and increased risk of frequent flooding (including the ‘York flood’ in November 2000). This could be one explanation for the higher negative values for annual percentage changes in the runoff in the region. The changes in annual runoff results from different input scenarios indicate that the catchment is highly sensitive to climate change especially to change in the

precipitation. The annual variation of runoff in corresponding to baseline flow for CCCMA and HadCM3 daring A2a scenario are shown in the Table 7 along with their equivalent months which showing upper and lower runoff values in each time slices. As it is shown in the Table, there is definite decrease in runoff during A2a scenarios in both GCMs in all study time slices. In the case of CCCMA, the annual percentage change values are lower in 2050s than that in 2020s and in 2080s. An opposite annual tread has been observed in the case HadCM3; it has shown a higher percentage change value in 2050s and a lower value in 2080s in comparison to that of 2020s (Table 7). It is important to note that annual values close to the higher valued changes in summer/autumn seasons and tend to hide variations in the other seasons. These values give an impression that flood risk in the region in remainder of 21st century may not exceed that experienced during the period of 1999-2008; but flood risk related representations would be clearer only when we adopt low time scale data (e.g. daily/ hourly) for modelling.

In other words, the climate change impact on regional hydrology could easily be assessed by comparing the variations in annual average runoff under different scenarios. The annual average runoff values and percentage changes under A2a scenario are 16.86 m^3/s (-15.28 %), 17.49 m^3/s (-12.08 %), 16.75 m^3/s (-15.8 %) respectively based on CCCMA-A2a GCM results during the 2020s, 2050s and 2080s respectively. The annual average runoff values and percentage changes in runoff for HadCM3-A2a scenario are 16.70 m^3/s (-16.06 %), 16.22 m^3/s (-18.49 %) and 17.56 m^3/s (-11.67 %) during 2020s, 2050s and 2080s respectively. The CCCMA-A2a suggests that 2050s has got lowest percentage change among all three time slices and this value is close to the percentage changes suggested by HadCM3-A2a in 2080s. However, the tabulated changes in annual effective runoff appear to be large in the A2a (medium to high emissions) scenario. It is interesting to note that there is potential chance of

variability in high runoff months in 2080s during A2a scenario (Table 7). The CCCMA-2080s suggests the higher runoff month is February whereas the HadCM3-2080s outputs show there is a chance of higher runoff shift from January to March. In all other time slices, both GCMs have shown same trend predicting higher runoff month as January and the month with low runoff month as July. Given the indications for substantial shift in higher runoff moths, it hints to the possibility of high intensity precipitation in early months of spring during A2a scenarios in 2080s.

3.3.2 B2a Scenario

This section explains the hydrological modelled results under the B2a scenario and compares the stream flow simulated by monthly time-step auxiliary - HyMOD using GCM outputs from CCCMA and HadCM3 models for the 2020s, 2050s and 2080s with observed stream flow for recent 10 years (1999-2008). The pictorial representations of variation of runoff in Derwent River, suggested by SRES B2a CCCMA model during three time slices are shown in the Figure 13. The corresponding runoff changes as per SRES B2a HadCM3 model is shown in the Figure 14. The uncertainty bounds associated with runoff simulations in each month can found in the Figure 13 and Figure 14; and those figures show higher uncertainty bounds during winter and spring season and lower bounds during summer and autumn seasons, in both GCMs. This variation in uncertainty in B2a scenario is synonymous to that of A2a scenario. The annual runoff changes in B2a scenarios during 2020s, 2050s and 2080s are shown in the Table 7. The anticipated average annual discharge in the catchment during 2020s was estimated as 17.75 m^3/s (353.03 mm/ year) as per CCCMA-B2a scenario, which is nearly -10.76% lesser than the corresponding values during 1999-2008 period (19.89 m3/s [395.62 mm/year]). The corresponding CCCMA-B2a based annual values estimated for time slices like the 2050s and 2080s are 15.92 m3/s (316.54 mm/ year) [which is -19.99% from baseline annual average runoff value] , and 18.23 m3/s (362.63 mm/year) [and which is -

8.34 % change from baseline annual average runoff value]. It is interesting to note that the runoff values in the Derwent catchment is expected to be lower in 2050s than that of the 2080s in the case of CCCMA-B2a forcing scenario. In comparison to A2a and B2a scenario results from CCCMA model, one can deduce that the annual runoff reduction is less in 2080s in comparison to other study periods in B2a scenario; whereas in the case of A2a a scenario runoff reduction values for 2080s remains relatively same as that of 2020s in Derwent river basin.

Simulations based on CCCMA-B2a GCM results showed an increase of +17.40 % in December runoff in 2020s, -4.19% in 2050s and +115.37% in 2080s ; whereas the corresponding values by HadCM3-B2a are -5.46%, 18.71%, and 4.11% respectively in 2020s, 2050s and 2080s. When the change in runoff is viewed as a percentage change from the earlier period, in the case of HadCM3-B2a emission scenario, the simulated annual average runoff in 2020s is 16.74 m^3/s (332.79 mm/year), -15.88% lower than the baseline discharge value. The HadCM3-B2a simulated annual runoff during 2050s and 2080s shows that those values are larger than that of calculated runoff during 2020s, so the percentage reduction in 2050s and 2080s are comparatively smaller than 2020s. The annual runoff value during 2050s is 17.44m3/s (346.76 mm/year), a -12.36% reduction in runoff as compared to the 1999-2008 baseline period. The corresponding value during 2050s was 17.30 m3/s (344.03 mm/year), a -13.04% reduction from the baseline annual average runoff value of 19.89 m3/s [395.62 mm/year]. If we compare B2a and A2a scenario outputs of HadCM3 model, we can note that the annual reduction value in 2080s is smaller than that that in 2020s in both scenarios. In the case of 2050s, HadCM3 has shown contradicting results with higher values of annual runoff reductions during A2a and lower reductions during B2a in comparison to 2020s and 2080s.

3.4 Seasonal Changes in Fluvial Hydrology

3.4.1 A2a Scenario

Figure 15 shows the percentage change of runoff in different seasons for the three time horizons considered for this study based on SRES A2a CCCMA and HadCM3. Figure 15(a) shows the winter season. In this season, CCCMA-simulations suggest an average decrease in runoff by the 2020s, which changes to a relative increase in the 2050s and a slight decrease by the 2080s. In comparison to the CCCMA model, the HadCM3 based simulations give higher percentage reductions. Even though, the mean predicted changes are negative, the upper uncertainty bounds extend into positive changes in runoff, indicating high uncertainty to positive ranges during the winter seasons. The pictorial percentage mean precipitations during different seasons in the study area for the period of 2020s, 2050s and 2080s are shown in the Figure 15 as obtained from both CCCMA and HadCM3 models during A2a scenario.

In the spring season (Figure 15(b) CCCMA simulated runoff is decreases through the 2080s while both increases (in 2080s) and decreases (in 2050s) are simulated by the HadCM3 simulation. HadCM3 suggests decreases in spring runoff by the 2020s, and a slightly larger decrease by the 2050s. As a result of the increase of seasonal precipitation amounts (for the spring period as per HadCM3) in the 2080s, mean spring runoff variations for Derwent have recently become positive. A substantial reduction in summer runoff was observed for simulations driven by both GCMs (figure 15(c)). However, in the case of HadCM3, lesser reductions are observed in 2080s than in the 2050s, relative to the baseline period.

Figure 15(d) shows percentage changes in runoff for the autumn months along with corresponding changes in precipitation. It is interesting to note that the drying pattern of autumn season same as that of the summer season, but with higher values of percentage

changes. CCCMA based simulation gives a percentage reduction of autumn runoff and which is higher than that of the summer months during the 2020s and 2080s while the HadCM3 based simulation shows that percentage reduction in autumn runoff exceeds that of the summer runoff during 2050s and 2080s. In 2020s, the CCCMA based simulation has shown a mean autumn runoff reduction of -32.68% and the modelled uncertainty ranging from +10.41% to -51.03%; meanwhile the HadCM3 based simulation has shown a mean value and uncertainty bound of -28.96% and (+13.90%, -49.46%). Similar responses were observed in the 2050s. Such considerable reductions on runoff and stream-flow regimes during summer and autumn in relation to climate change scenarios may cause potential impacts like reductions in water quality of the river and high human, environmental and industrial demands for water supplies. The observed changes in autumn season are also very significant for the river basin's groundwater recharge and storage. The most significant changes were observed for the 2080s for both GCM driven simulations with mean reduction in runoff of -34.09% for CCCMA and -34.84% for HadCM3 respectively. In this study climate change scenarios show declines in summer and autumn precipitation in the region which could result in significant declines in summer and autumn runoff in these regions. The drastic declining nature of runoff could also connected to possible chances of declination in summer/autumn soil-moisture levels.

In general both GCMs have shown relatively similar results in the drier seasons of summer and autumn, while the effect of GCM uncertainty is more prominent during the wetter seasons of winter and spring. The HadCM3 based future scenario (A2a) for the 2080s indicates changes in winter stream flow of -1.48% with upper and lower uncertainty bounds (including hydrological model uncertainty) of (+52.88%, -31.69%) and summer reductions of up to -31.07% in comparison to baseline comparing period (1999-2008). It was interesting to note that prominent increase in runoff during winter season exhibited only towards the end

of the season (February) in both HadCM3 and CCCMA GCMs during all three study periods (2020s, 2050s and 2080s). The reasons for lower values of percentage reductions could be connected to the peculiar feature of the baseline period for comparison (1999-2008) with high intensity of extreme floods. Lane (2002) showed the evidence of increases in the number and extent of runoff in Yorkshire region during these periods. Fowler and Kilsby (2003) have observed that multiday extreme rainfall events in Yorkshire have become more frequent during 1991-2000 in comparison to period 1961-1990 with the average recurrence interval for a 50 year event drastically changing to only 25 years. Our winter results indirectly indicate that the future risk of flood events in Yorkshire region would be lesser than that of 1999-2008 periods during winter months like December and January but the risk is greater during the later month of winter (February) during time periods like 2020s, 2050s and 2080s. Even though the mean percentage change values are negatives in earlier months of the winter seasons, the largest uncertainty bounds in winter season months indicates that results are highly sensitive to the local climate. The Derwent catchment has also showed reductions in autumn and spring, which are critical recharge periods in groundwater point of view of the region. It indicates need of efficient water resources management strategies to counter its effect on groundwater aquifer, local water industries, local water treatments and dilution of wastewater effluent, agricultural and ecological water demands and management.

3.4.2 B2a Scenario

This study also evaluates the seasonal comparison of HadCM3 and CCCMA models under the B2a scenario. The Figure 16 shows the percentage change of runoff and precipitation in different seasons for the three time horizons considered for this study based on SRES B2a CCCMA and HadCM3. The Figure 16(a) shows the variations during the winter season during 2020s, 2050s and 2080s in comparison to 1999-2008 periods. The analysis result has shown that both GCMs during B2a scenario have given contradicting results during winter

season of 2020s and 2050s. The CCCMA-B2a based simulation has shown a mean winter runoff change of +3.52% and the modelled uncertainty ranging from + 75.01% to -34.91% meanwhile the HadCM3-B2a based simulation has shown a mean value and uncertainty bound of -5.20% and (+62.99%, -42.22%) during 2020s. In the case of 2050s, the CCCMA-B2a has produced a percentage change of -12.83% with uncertainty bounds of [+41.88%, -41.42%]; and the corresponding runoff change produced by HadCM-B2a was 6.52% with uncertainty bounds of [+74.24%, -32.82%]. Both the GCMs have produced similar trend during winter season of 2080s with moderate increases in mean runoff with values of +3.71% and +2.16% for CCCMA-B2a and HadCM3-B2a respectively. The corresponding uncertainty bounds during winter seasons of 2080s are [+56.79%, -39.75%] and [+65.87%, -33.74%] for CCCMA-B2a and HadCM3-B2a respectively. Whilst GCMs simulate decreases in precipitation with climate change for the all seasons except winter, there is no GCM consensus in the sign of precipitation and modelled runoff change in the Derwent catchment for the winter seasons of the B2a simulated periods.

The percentage changes in runoff during spring seasons of study periods are shown in the Figure 16(b) along with that of GCM suggested precipitation changes in different seasons. Apart from winter seasons, there is an agreement between the CCCMA and HadCM3 in B2a scenario that runoff decreases with global warming for the Derwent Basin. The visual comparison of variation of precipitation and runoff in different time domains in the Figure 16 has shown reasonable linear relationship between downscaled precipitation and modelled runoff values and it is quite obvious as runoff is simply the area-normalized difference between precipitation and evapotranspiration with a nonlinear component of watershed characteristics function. The results indicate that the CCCMA-B2a has produced a percentage reduction of -2.38% with uncertainty bounds of [+57.62%, -41.02%]; the corresponding change by HadCM3-B2a is -9.15% [+48.07%, -44.04%] during 2020s. In the case of

CCCMA-B2a, the anticipated average changes in runoff are -11.42% and -3.55% respectively during 2050s and 2080s with uncertainty bounds of [43.58%, -46.17%] and [163.76%, -45.51%] respectively. In the case of HadCM3-B2a the corresponding values are -6.97% [51.64, -43.16%] and -1.59% [58.96, -39.63%] respectively. The mean percentage changes in precipitation during three time slices are 0.99%, -6.74% and -5.39% as per CCCMA-B2a; and the corresponding changes suggested by HadCM3-B2a are -7.16%, -5.19% and 4.01% during 202s, 2050s and 2080 s respectively. In comparison to spring season of A2a scenario, one noticeable difference is occurred in the runoff estimated from the HadCM3 outputs of 2080s time slice with increase percentage change in runoff value in A2a scenario with a value of +3.94%. Looking into monthly variations of A2a and B2a (Table 7), one can suspect that there is considerable inter-annual variability in both the magnitude and timing of spring runoff in the Derwent basin. However, proper evaluation of such variable nature is possible only through analysing high temporal resolution data sets.

In comparison to calculated runoff values at A2a scenario, the percentage runoff reduction values at B2a scenario have shown a steady increasing trend in both summer and autumn seasons. The GCM expected reduction in summer runoff is higher in the B2a scenario than that of A2a in the case of both the models (Figure 16(c)). The B2a autumn seasonal variation of precipitation and runoff at the Derwent river catchment is shown in the Figure 16(d). The results have shown that the mean precipitation during autumn season in 2020s is 70.27mm (average of September, October and November) and the CCCMA-B2a and HadCM3-B2a values are 15.06% and 12.47% smaller than this value. The autumn runoff reduction predicted by CCCMA model in B2a scenario is larger than CCCMA-A2a scenario during 2050s. In the case of HadCM3 model during B2A scenario, more drying is expected during 2020s; while the drying situation is fairly similar during 2050s and 2080s. In general, from Figures 15(a-d) and 16(a-d), the variability in precipitation and runoff between two GCMs

under B2a and A2a scenario are evident with a clear undulation tendency in winter and spring seasons for both scenarios. As per the simulation results and GCM data sets, the greater influence of climatic changes is exerted on variations of seasonal and monthly runoff which results in predominantly negative runoff variations for the summer and autumn period and slightly positive trends in certain winter and spring months of the study slices over the Upper Derwent catchment. The lowering trend of runoff during summer and autumn seasons could be connected with projected rising temperature, potential evapotranspiration and variability in precipitation by the middle and the end of this century.

4. Discussions and Conclusions

The primary target of this study was to demonstrate the linking of standard, readily available, spatially downscaled GCM data at the monthly timescale with a properly calibrated monthly hydrological model to perform a seasonal hydrological climate-change impact assessment for one of the major river catchments (River Derwent upper catchment) in the Yorkshire and Humber region of Northern England. A conceptual rainfall-runoff model operating at a monthly time-step (auxiliary HyMOD) has been driven using spatially downscaled (~5km) monthly precipitation, temperature and potential evaporation (obtained from Blaney-Criddle method) data from two major general circulation models: CCCMA and HadCM3, and two driving scenarios: A2a and B2a. A Monte-Carlo approach based SCEM-UA algorithm (which allows the inclusion of parameter uncertainty) has been used to calibrate the HyMOD using UKCP09 and UK National River Flow Archive data from October 1973 to December 2006.

While the monthly time-step auxiliary model succeeded in capturing the stream flow distribution fairly well when driven by UKCP09 historical monthly data from the study area, there was an indication of underestimation of the discharge in wet seasons such as winter in a number of years containing heavy intensity of extreme discharge events. However, a

comparison of the monthly model outputs to observed data has showed that the monthly model actually performed well in the low-flow drier seasons of summer and autumn. The incorporation of a bias correction method enabled the system to simulate stream flow values of months with extreme events (50 year return period and more) to reasonable level of accuracy.

A further aim of the study was to identify the disparity in different GCM outputs when combined with conceptual hydrological models to simulate the future distribution of monthly and seasonal river flows, Comparing the performance of two GCMs, both CCCMA and HadCM3 predict similar steam flow changes for summer and autumn under both A2a and B2a scenarios. However, significant disparities are observed for winter and spring. During winter and spring, HadCM3-A2a predicts a significant increase in runoff from the 2050s to the 2080s whereas the CCCMA-A2a simulates a decrease in flow during 2080s in comparison to 2050s during both seasons. For the B2a scenario, both CCCMA and HadCM3 show similar trends in variation during spring seasons with high difference in numerical values. Stream flows from the two models interestingly contradicting each other for the B2a winter season due to large differences in predicted precipitation. Another notable divergence is associated with spring in the 2080s. The months of March and May in the 2080s period show an increase in runoff with values of +13.4% and +2.24% respectively for HadCM3-A2a, whereas CCCMA show negative values with a large uncertainty spanning ~(+60% , -40%). In general, the systematic ensemble simulation results (with hydrological uncertainty) clearly showed a trend of projected future flows decreasing nearly in all months except winter. Summer and autumn flows experience a greater relative change under both A2a and B2a scenarios for both GCMs, with predicted changes less than those derived by Cloke et al (2010) for the Medway catchment with CATCHMOD model. Monthly and seasonal uncertainty bounds are wide as we have considered parameter uncertainty and spatial

variation of atmospheric variable values of GCMs through systematic ensembles of inputs while simulating the model. This study has demonstrated a variation of peak runoff months in 2080s (from January to February in the case of CCCMA and January to March in the case of HadCM3) during A2a scenarios. Such phenomenon of substantial increase flow in spring months are observed in the case of other UK catchments (Arnell et al., 1990; Arnell and Reynard, 1993; Boorman and Sefton, 1997). A detailed study by Limbrick et al (2000) suggested that flows were especially increased during spring season as a result of the flow distribution characteristics of the baseline years.

The monthly and seasonal results obtained from this study are largely in line with previous work conducted in both Britain and Ireland with slight disparity in the winter simulations. Based on HadRM3H regional climate model [SRES A2 (UKCIP02 Medium-High) scenario] based climate change stimulated hydrological impact assessment on few catchments in northwest England, Fowler and Kilsby (2007) concluded that the climate change impacts on monthly flow distribution of the northwest region of England are very significant, with summer reductions of 40–80% of 1961–90 mean flow, and winter increases of up to 20%. The results of this investigation with the use of spatially downscaled GCM data in monthly time step suggests that different GCMs in both B2a and A2a scenarios, give comparable results in drier seasons like summer and autumn and considerable variations during seasons like winter and spring.

Though, the findings in this article could be useful for other environmental impact adaptation studies in the region, there are a number of additional factors that could be incorporated into future studies. Murphy et al. (2006) highlight the need to address the ‘cascade’ of uncertainty associated with climate impact studies. The propagation of uncertainties from GCM to regional hydrology stem from a hierarchy of sources and conditions: forcing scenarios, use of different GCMs, different realizations of a given scenarios in different GCMs, method of

downscaling, forcing and processes in GCM sub-grid etc. (Liu et al., 2010). This regional hydrological impact study focused on single realization of two GCM for two IPCC emission scenarios. Though, different systematic ensembles of data sets used for the future hydrological modelling, other sources of uncertainty should be considered in the future to improve confidence in quantified connection between climate change and regional fluvial hydrology. Fowler (2005) has shown that there is evidence of a significant positive trend in rainfall intensity in the UK but no evidence of a similar increase in flooding at the national level, except few Yorkshire regional studies (Lane, 2002). Fowler (2005) noted that Yorkshire floods are product of complex interaction of the spatial-temporal rainfall pattern, hydrological connectivity of the catchments and river conveyance capability and effective tackling or prediction would require clear understanding of links between flood generating mechanisms (through hydrological models), atmospheric circulation patterns (climatic models) and land management practices.

Though this study focused on monthly conceptual model, we can't avoid the influence of land use on hydrological processes. Due to many facts, the identification and quantification of the variation of the hydrology with land-use change are complicated procedure but which are critical in daily time step modelling (DeFries and Eshleman, 2004). Turner et al (2003) highlights the need to focus on land use to study the consequences of anthropologic and climate change on hydrology. Rounsevell and Reay (2009) review the relationships between land use and climate change in UK perspective. Zhu *et al.* (2005) discuss the inadequacy of models to explain the trends in stream flow at 47 streams in Pennsylvania with climate alone. This study has clearly emphasised the need to incorporate land use effects in hydrological modelling. Daily time step semi distributed models like Soil Water Assessment Tool (SWAT) have recently gained considerable attention on and use and climate change impacts on the hydrology (Mango et al., 2011). Dunn and Mackay (1995) has used a catchment model

to demonstrate the direct effect of land use on hydrology through its link with the evapotranspiration.

Nevertheless this work presented as a case study at a catchment scale, further enhancement of this study are planned to come up with more semi distributed hydrological models like SWAT (which can consider changes in land use) and more realistic representation of the uncertainties suitable for various beneficiary workgroups like insurance, business, economists and planners considering more GCMs/RCMs and suitable hydrological models under different IPCC scenarios. However, this study does provide a baseline demonstration of the type of results that may be obtained using readily available monthly GCM datasets utilizing properly biased corrected monthly conceptual hydrological models.

5. Acknowledgements

This study was funded by Yorkshire Forward within the research project 'Low Carbon and Climate Resilient Regional Economy' which has the objective of a assessing the impacts of climate change on resources that influences future regional economy of the Yorkshire – Humberside region of the North-East England. Authors also would like to express sincere thanks to Met Office and Environmental Agency of UK for providing required data. The authors wish to thank the WorldClim data portal and International Centre for Tropical Agriculture (CIAT) climate change downscaled data portal for providing required data sets.

6. References

Arnell NW. 1992. Factors controlling the effects of climate change on river flow regimes in humid temperature environment. *Journal of Hydrology* **132**: 321–342.

Arnell NW. 2003. Effects of Climate Change on River Flows and Groundwater Recharge Using the UKCIP02 Scenarios. Report to UK Water Industry Research Limited, University of Southampton, UK.

Abaurrea J, As´ın J. 2005. Forecasting local daily precipitation patterns in a climate change scenario. *Climate Research* **28**: 183–197.

Arnell NW, Brown RPC, Reynard N. 1990. Impact of climatic variability and change on river flow regimes in the UK. Institute of Hydrology Report No. 107: 154.

Arnell NW, Reynard N. 1993. Impact of climate change on river flow regimes in the United Kingdom. Institute of Hydrology Report to DOE, Water Directorate.

Berga P, Feldmanna H, Panitza H.-J. 2012. Biascorrection of high resolution regional climate model data. *Journal of Hydrology* **448–449**: 80–92.

Bergant K, Kajfez-Bogataj L. 2005. N-PLS regression as empirical downscaling tool in climate change studies. *Theoretical and Applied Climatology* **81**: 11–23.

Boorman DB, Sefton CEM. 1997. Recognising the uncertainty in the quantification of the effects of climate change on hydrological response. *Climatic Change* **35**: 415-434.

Blaney HF, Criddle WD. 1950. Determining Water Requirements in Irrigated Areas from Climatological Irrigation Data. Technical Paper No. 96, US Department of Agriculture, Soil Conservation Service, Washington, D.C: 48

Boyle DP. 2000. Multicriteria calibration of hydrological models. PhD Dissertation, Dep of Hydrol and Water Resour, Univ of Arizona, Tucson

Box GEP, Tiao GC. 1973. Bayesian inference in statistical analysis. Addison-Wesley, Reading, MA.

Brower C, Heibloem M. 1986. Irrigation water management: Irrigation water needs, Training Manual 3, FAO, Rome.

Cameron D. 2006. An application of the UKCIP02 climate change scenarios to flood estimation by continuous simulation for a gauged catchment in the northeast of Scotland, UK (with uncertainty). *Journal of Hydrology* **328**: 212–226.

Christensen JH, Carter TR, Rummukainen M, Amanatidis G. 2007. Evaluating the performance and utility of regional climate models: the PRUDENCE project. *Climatic Change* **81**: 1–6.

Cleveland W. 1979. Robust locally weighted regression and smoothing scatterplots. *J. Amer. Stat. Assoc* **74**: 829–839.

Cloke HL, Jeffers C, Wetterhall F, Byrne T, Lowe J, Pappenberger F. 2010. Climate impacts on river flow: projections for the Medway catchment, UK, with UKCP09 and CATCHMOD. *Hydrol. Process*. DOI: 10.1002/hyp.7769.

DeFries R, Eshleman KN. 2004. Land-use change and hydrologic processes: a major focus for the future. *Hydrol. Process* **18**: 2183–2186.

Diaz-Nieto J, Wilby R.L. 2005. A comparison of statistical downscaling and climate change factor methods: Impacts on low flows in the River Thames, United Kingdom. *Climatic Change* **69**: 245–268.

Duan Q, Gupta VK, Sorooshian S. 1992. Effective and efficient global optimization for conceptual rainfall–runoff models. *Water Resour. Res* **28**: 1015–1031.

Dunn SM, Mackay R. 1995. Spatial variation in evapotranspiration and the influence of land use on catchment hydrology. *Journal of Hydrology* **171**: 49-73.

Enke W, Schneider F, Deuschlander T. 2005. A novel scheme to derive optimized circulation pattern classifications for downscaling and forecast purposes. *Theoretical and Applied Climatology* **82**: 51–63.

FORESIGHT. 2004. Future Flooding Executive Summary. Office of Science and Technology, HMSO: London: 59.

Fowler HJ, Kilsby CG. 2003. A regional frequency analysis of United Kingdom extreme rainfall from 1961 to 2000. *International Journal of Climatology* **23**: 1313–1334.

Fowler H. 2005. Are extremes increasing? Changing rainfall patterns in Yorkshire. *The Yorkshire and Humber Regional Review Spring* **15(1):** 29-31.

Fowler HJ, Ekstr¨om M, Kilsby CG, Jones PD. 2005a. New estimates of future changes in extreme rainfall across the UK using regional climate model integrations. 1: assessment of control climate. *J Hydrol* **300**: 212–233.

Fowler HJ, Kilsby CG, O'Connell PE, Burton A. 2005b. A weather type conditioned multi-site stochastic rainfall model for generation of scenarios of climatic variability and change. *J Hydrol* **308(1–4)**: 50–66.

Fowler HJ, Kilsby CG. 2007. Using regional climate model data to simulate historical and future river flows in northwest England. *Clim Change* **80**: 337–367.

Fowler HJ, Blenkinsopa S, Tebaldib C. 2007. Linking climate change modelling to impacts studies: recent advances in downscaling techniques for hydrological modelling. *Int. J. Climatol.* **27**: 1547–1578.

Fowler HJ, Tebaldi C, Blenkinsop S. 2008. Probabilistic estimates of climate change impacts on flows in the River Eden, Cumbria. In: Sustainable Hydrology for the 21st Century, Proc. 10th BHS National Hydrology Symposium, Exeter: 416–423.

Fuller RM, Smith GM, Sanderson JM, Hill RA, Thompson AG. 2002. The UK land cover map 2000: construction of a parcel-based vector map from satellite images. *Cartographic Journal* **39**: 15–25.

Gelman A, Rubin DB. 1992. Inference from iterative simulation using multiple sequences. Stat. Sci 7: 457– 472.

Graham LP, Andréasson J, Carlsson B. 2007a. Assessing climate change impacts on hydrology from an ensemble of regional climate models, model scales and linking methods - A case study on the Lule River basin. *Climatic Change* **81**(Supplement): 293–307.

Harman J, Bramley ME, Funnell M. 2002. Sustainable flood defence in England and Wales. Civil Engineering, "Floods – A new Approach". 150 (1): 3-9.

Hashino T, Bradley AA, Schwartz SS. 2006. Evaluation of bias-correction methods for ensemble stream flow volume forecasts. *Hydrol. Earth Syst. Sci. Discuss* **3**: 561–594.

Hijmans RJ, Cameron SE, Parra JL, Jones PG, Jarvis A. 2005. Very high resolution interpolated climate surfaces for global land areas. *International Journal of Climatology* 25: 1965–1978.

Holland J. 1975. Adaptation in Natural and Artificial Systems, Univ. of Mich. Press, Ann Arbor, Mich.

Hulme M, Jenkins GJ, Lu X, Turnpenny JR, Mitchell TD, Jones RG, Lowe J, Murph JM, Hassell D, Boorman P, McDonald R, Hill S. 2002. Climate Change Scenarios for the United Kingdom: The UKCIP02 Scientific Report, Tyndall Centre for Climate Change Research, School of Environmental Sciences, University of East Anglia, Norwich, UK: 120

Hutchins MG, Deflandre-Vlandas A, Posen PE, Davies HN, Colin, N, 2010. How Do River Nitrate Concentrations Respond to Changes in Land-use? A Modelling Case Study of Headwaters in the River Derwent Catchment, North Yorkshire, UK. *Environ Model Assess.* **15(2)**: 93–109.

Jiang T, Chen YD, Xu C, Chen X, Chen X, Singh VP. 2007. Comparison of hydrological impacts of climate change simulated by six hydrological models in the Dongjiang Basin, South China. *Journal of Hydrology* **336**: 316–333.

Kay AL, Jones RG, Reynard NS. 2006a. RCM rainfall for UK flood frequency estimation. I. Method and validation. *Journal of Hydrology* **318**: 151–162.

Kay AL, Jones RG, Reynard NS. 2006b. RCM rainfall for UK flood frequency estimation. II. Climate change results. *Journal of Hydrology* 318: 163–172.

Kay AL, Davies HN, Bell VA, Jones RG. 2009. Comparison of uncertainty sources for climate change impacts: flood frequency in England. *Climatic Change* 92: 41–63 DOI 10.1007/s10584-008-9471-4

Lane SN. 2002. More floods, less rain: changing hydrology in a Yorkshire context, The *Yorkshire and Humber Regional Review* 11(3): 18–19.

Leckebusch GC, Ulbrich U. 2004. On the relationship between cyclones and extreme windstorm events over Europe under climate change. *Global and Planetary Change* 44: 181–193.

Leung LR, Hamlet AF, Lettenmaier DP, Kumar A. 1999. Simulations of the ENSO hydroclimate signals in the Pacific Northwest Columbia River basin. Bull. Amer. *Meteorol. Soc* 80: 2313–2328.

Limbricka KJ, Whitehead PG, Butterfieldb D, Reynardc N. 2000. Assessing the potential impacts of various climate change scenarios on the hydrological regime of the River Kennet at Theale, Berkshire, south-central England, UK: an application and evaluation of the new semi-distributed model, INCA. *The Science of the Total Environment* 251/252 2000 539-555

Liu Z, Xu Z, Huang J, Charles SP, Fu G. 2010. Impacts of climate change on hydrological processes in the headwater catchment of the Tarim River basin, China. *Hydrol. Process*. 24: 196–208.

Mango LM, Melesse AM, McClain ME, Gann D, Setegn G. 2011. Land use and climate change impacts on the hydrology of the upper Mara River Basin, Kenya: results of a modeling study to support better resource management. *Hydrol. Earth Syst. Sci* 15: 2245–2258.

Mearns LO, the NARCCAP Team. 2006. Overview of the North American Regional Climate Change Assessment Program. In NOAA RISA-NCAR Meeting, Tucson, AZ, March.

Metropolis N, Rosenbluth AW, Rosenbluth MN, Teller AH, Teller E. 1953. Equations of state calculations by fast computing machines. *J. Chem. Phys.* 21: 1087–1091.

Moore RJ. 1985. The probability-distributed principle and runoff production at point and basin scales. *Hydrol Sci J* 30(2): 273–297.

Moradkhani H, Sorooshian S, Gupta HV, Houser PR. 2005. Dual state–parameter estimation of hydrological models using ensemble Kalman filter. *Advances in Water Resources* 28: 135–147.

Murphy AH, Winkler RL. 1987. A general framework for forecast verification. Mon. *Wea. Rev* 115: 1330–1338.

Murphy C, Fealy R, Charlton R, Sweeney J. 2006. The reliability of an 'off-the-shelf' conceptual rainfall runoff model for use in climate impact assessment: uncertainty quantification using Latin hypercube sampling. *Area* 38.1: 65–78.

Panagoulia D, Dimou G. 1997a. Linking space-time scale in hydrological modelling with respect to global climate change. Part 1. Models, model properties, and experimental design. *Journal of Hydrology* 194: 15–37.

Panagoulia D, Dimou G. 1997b. Linking space-time scale in hydrological modelling with respect to global climate change. Part 2. Hydrological response for alternative climates. *Journal of Hydrology* 194: 38–63.

Parker DE, Legg TP, Folland CK. 1992. A new daily central England temperature series, 1772–1991. *Int J Climatol* 12: 317–342.

Pilling C, Jones JAA. 1999. High resolution equilibrium and transient climate change scenario implications for British runoff. *Hydrol. Proc* 13(17): 2877-2895.

Pilling CG, Jones JAA. 2002. The impact of future climate change on seasonal discharge, hydrological processes and extreme flows in the Upper Wye experimental catchment, mid-Wales. *Hydrol Process* 16: 1201–1213.

Price WL. 1987. Global optimization algorithms for a CAD workstation, J. Optim. *Theory Appl* 55(1): 133– 146.

Prudhomme C, Reynard N. Crooks S. 2002. Downscaling of global climate models for flood frequency analysis: where are we now? *Hydrological Processes* 16: 1137-1150.

Ramirez J, Jarvis A. 2010. Downscaling global circulation model outputs: The Delta method, Decision and Policy Analysis Working Paper No 1: CIAT-CGIAR: 1 – 18.

Reynard NS, Prudhomme C, Crooks SM. 2001. The flood characteristics of large UK rivers: potential effects of changing climate and land use. *Climatic Change* 48: 343–359.

Rounsevell MDA, Reay DS. 2009. Land use and climate change in the UK. Land Use Policy 26S: S160–S169.

Schaeffli B, Gupta HV. 2007. Do Nash values have value? *Hydrologic Processes* 21(15): 2075–2080. DOI: 10·1002/hyp.6825.

Seibert J. 2001. On the need for benchmarks in hydrological modelling. *Hydrological Processes* 15: 1063–1064.

Smith JA, Day GN, Kane MD. 1992. Nonparametric framework for long-range stream flow forecasting. *J. Water Resour. Planning and Management* 118: 82–91.

Soetanto R, Proverbs DG. 2004. Impact of flood characteristics on damage caused to UK domestic properties: the perceptions of building surveyors. *Structural Survey* 22(2): 95–104.

Turner II BL, Matson PA, McCarthy J, Corell RW, Christensen L, Eckley N, Hoverlsrud-Broda GK, Kasperson JX, Kasperson RE, Luers A, Martello ML, Mathiesen S, Naylor R, Polsky C, Pulsipher A, Schiller A, Selin H, Tyler N. 2003. Illustrating the coupled human–

environment system for vulnerability analysis: three case studies. *Proceedings of the National Academies of Sciences* 100(14): 8080–8085.

Teutschbeina C, Seiberta J. 2012. Bias correction of regional climate model simulations for hydrological climate-change impact studies: Review and evaluation of different methods. *Journal of Hydrology* 456–457: 12–29.

Vrugt JA, Bouten W, Gupta HV, Sorooshian S. 2003a. Toward improved identifiably of hydrologic model parameters: the information content of experimental data. *Water Resour. Res* 39(3): 1054–1064.

Vrugt JA, Gupta HV, Bouten W, Sorooshian S. 2003b. A Shuffled Complex Evolution Metropolis algorithm for optimization and uncertainty assessment of hydrologic model parameters. *Water Resour. Res* 39(8): 1-16, doi:10.1029/2002WR001642.

Wagener T, Boyle DP, Lees MJ, Wheater HS, Gupta HV, Sorooshian S. 2001. A framework for development and application of hydrological models. *Hydrological and Earth Sciences* 5(1): 13–26.

Walsh CL, Kilsby CG. 2007. Implications of climate change on flow regime affecting Atlantic salmon. *Hydrology and Earth System Sciences* 11(3): 1127–1143.

Winsemius HC, Savenije HHG, Gerrits AMJ, Zapreeva EA, Klees R. 2006. Comparison of two model approaches in the Zambezi river basin with regard to model reliability and identifiability. *Hydrol. Earth Syst*. Sci 10: 339–352

Winsemius HC, Schaefli B, Montanari A, Savenije HHG. 2009. On the calibration of hydrological models in ungauged basins: A framework for integrating hard and soft hydrological information. *Water Resour. Res* 45: W12422, doi: 10.1029/2009WR007706.

Wood AW, Maurer EP, Kumar A, Lettenmaier DP. 2002. Long-range experimental hydrologic forecasting for the eastern United States. *J. Geophys. Res.-Atmos* 107: 4429 doi:10.1029/2001JD000659.

Xu CY, Halldin S. 1997. The Effect of climate change on river flow and snow cover in the NOPEX area simulated by a simple water balance model. *Nordic Hydrology* 28 (4/5): 273–282.

Xu CY, Singh VP. 1998. A review on monthly water balance models for water resources investigation and climatic impact assessment. *Water Resources Management* 12: 31–50.

Zhu Y, Day RL. 2005. Analysis of streamflow trends and the effects of climate in Pennsylvania, 1971 to 2001. *Journal of the American Water Resources Association* 41(6): 1393-1405.

List of Tables

List of Figures

Figure 1: The Location map of the study area, the River Derwent catchment

Figure 2. The seasonal variation of mean, maximum and minimum precipitation within the Upper Derwent catchment as obtained from different GCMs and Scenarios along with historical decadal mean precipitation values

Figure 3. The seasonal variation of mean, maximum and minimum daily annual temperature within the Upper Derwent catchment as obtained from different GCMs and Scenarios along with historical decadal mean, maximum and minimum values observed in catchment

Figure 4. The comparison of changes in seasonal monthly mean PET (estimated using Blaney-Criddle method) as obtained from CCCMA and HadCM3 Models (bias uncorrected) on the River Dewent catchment, Yorkshire-Humberside for study instants like 2020, 2050 and 2080 ((a): In the upper row the four maps show the average values of temperature (in ^{0}C) in seasons like spring, summer, autumn and winter as obtained from HadCM3 for the study instants 2020; (b): maps from CCCMA for the study instants 2020; (c): maps from HadCM3 for the study instants 2050; (d): maps from CCCMA for the study instants 2050; (e): maps from HadCM3 for the year 2080; (f): maps from CCCMA for the study instants 2080)

Figure 5. Display of distributions of the parameters and evolution of GR scale-reduction convergence diagnostic for the parameters in the auxiliary - HyMOD model using monthly runoff data from the River Derwent catchment and SCEM-UA (5(a) to 5(d) corresponds to parameters like Cmax, bexp, Alpha, Rs and Rq; 5(e) corresponds to variation of GR convergence diagnostic for these parameters)

Figure 6. Runoff forecasting by SCEM-UA parameter estimation of the auxiliary - HyMOD for the River Derwent Catchment ((shaded area with 95% uncertainty bound)

Figure 7. The scatter plot of performance of auxiliary-HyMOD under calibration data

Figure 8. The scatter plot of performance of auxiliary-HyMOD under validation data

Figure 9. Flood frequency curves derived from observed, auxilary - HyMOD modelled and auxilary - HyMOD modelled (bias corrected) mean flow time series at the River Derwent, Yorkshire-Humberside

Figure 10. The hydrological simulation results from different ensemble combinations of GCM data in Derwent catchment during 2050s [a). CCCMA-A2a, b). HadCM3-A2a]

Figure 11. Percentage change in mean monthly streamflow between the observed 1999-2008 period and future scenarios for 2020, 2050 and 2080 time-slices using the SRES A2a CCCMA Model, at the River Derwent catchment, Yorkshire-Humberside

Figure 12. Percentage change in mean monthly streamflow between the observed 1999-2008 period and future scenarios for 2020, 2050 and 2080 time-slices using the SRES A2a HadCM3 Model, at the River Derwent catchment, Yorkshire-Humberside

Figure 13. Percentage change in mean monthly streamflow between the observed 1999-2008 period and future scenarios for 2020, 2050 and 2080 time-slices using the SRES B2a CCCMA Model, at the River Derwent catchment, Yorkshire-Humberside

Figure 14. Percentage change in mean monthly streamflow between the observed 1999-2008 period and future scenarios for 2020, 2050 and 2080 time-slices using the SRES A2a HadCM3 Model, at the River Derwent catchment, Yorkshire-Humberside

Figure 15. Simulated percentage change in effective runoff in different seasons for each future time period considered (2020s, 2050s and 2080s) using SRES A2a CCCMA and HadCM3 forcing data , along with corresponding change in mean precipitation [(a) winter, (b) spring, (c) summer, (d) autumn] (NB: P corresponding to precipitation data and R corresponding to runoff data)

Figure 16. Simulated percentage change in effective runoff in different seasons for each future time period considered (2020s, 2050s and 2080s) using SRES A2a CCCMA and HadCM3 forcing data , along with corresponding change in mean precipitation [(a) winter,

1

(b) spring, (c) summer, (d) autumn] (NB: P corresponding to precipitation data and R corresponding to runoff data)

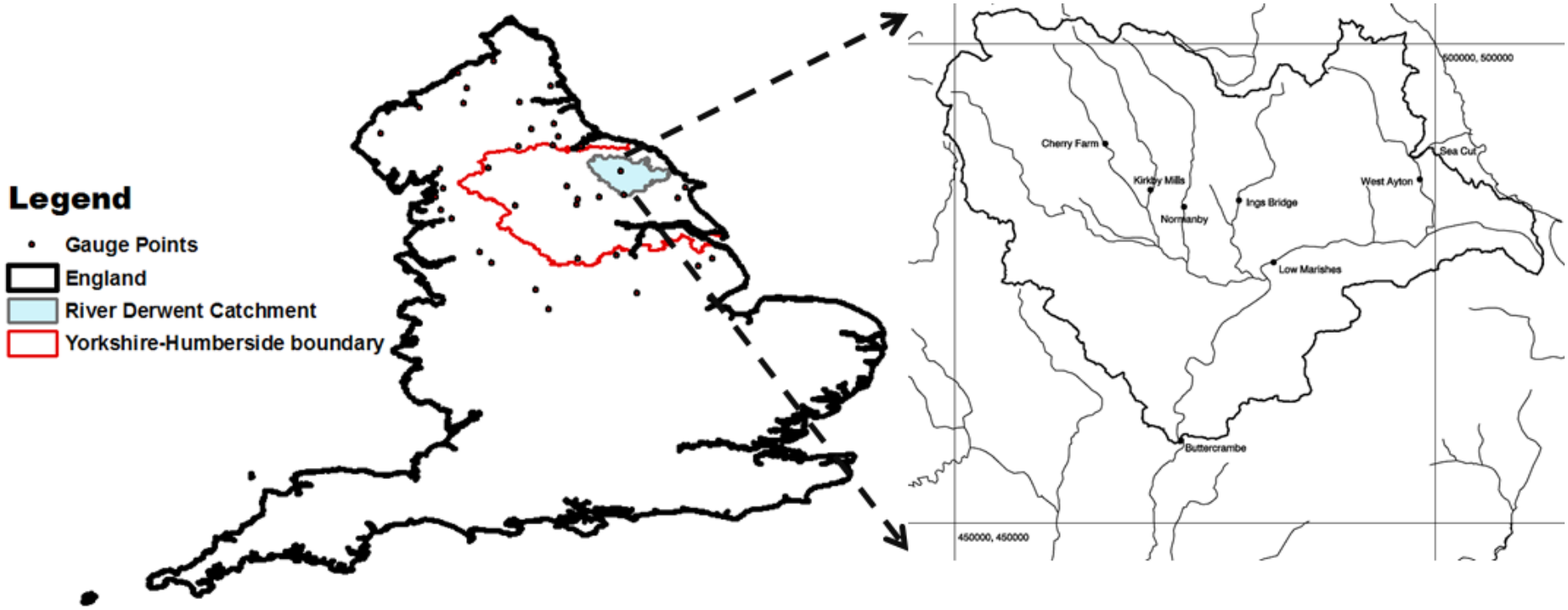

Figure 1: The Location map of the study area, the River Derwent catchment

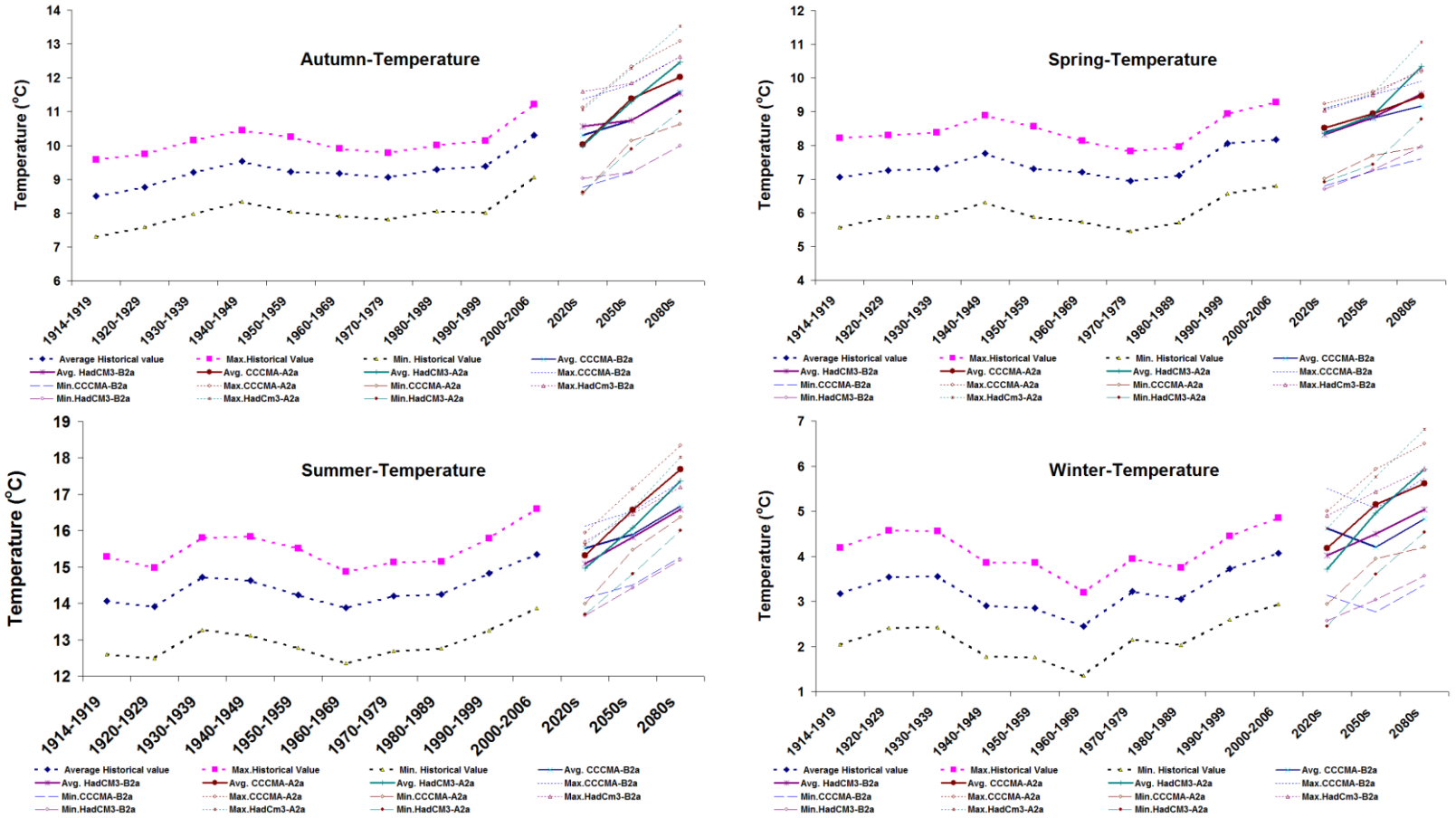

Figure 2. The seasonal variation of mean, maximum and minimum daily annual temperature within the Upper Derwent catchment as obtained from different GCMs and Scenarios along with historical decadal mean, maximum and minimum values observed in catchment (a) Autumn (b) Summer (c) Spring (d) Winter

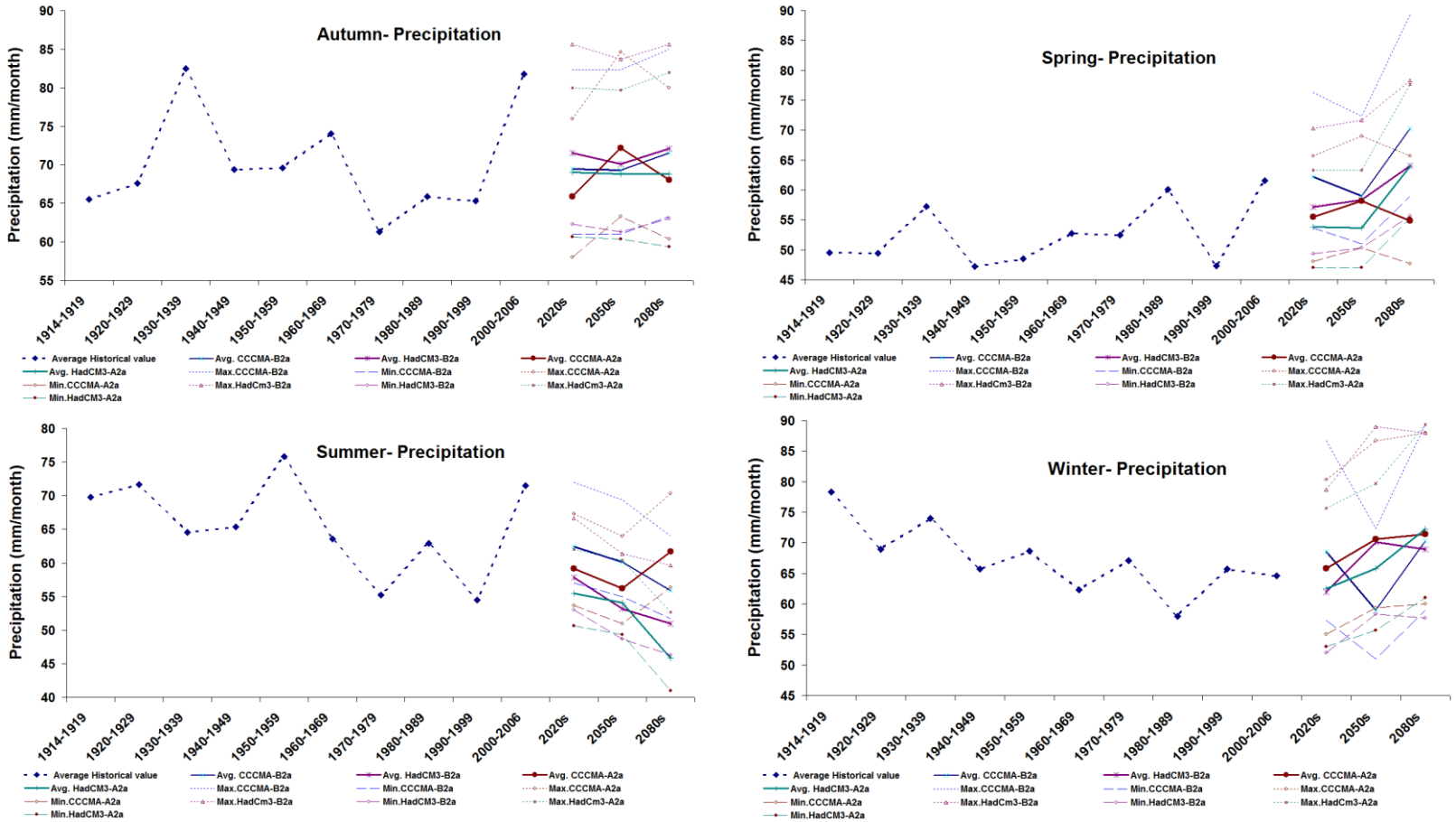

Figure 3. The seasonal variation of mean, maximum and minimum precipitation within the Upper Derwent catchment as obtained from different GCMs and Scenarios along with historical decadal mean precipitation values (a) Autumn (b) Summer (c) Spring (d) Winter

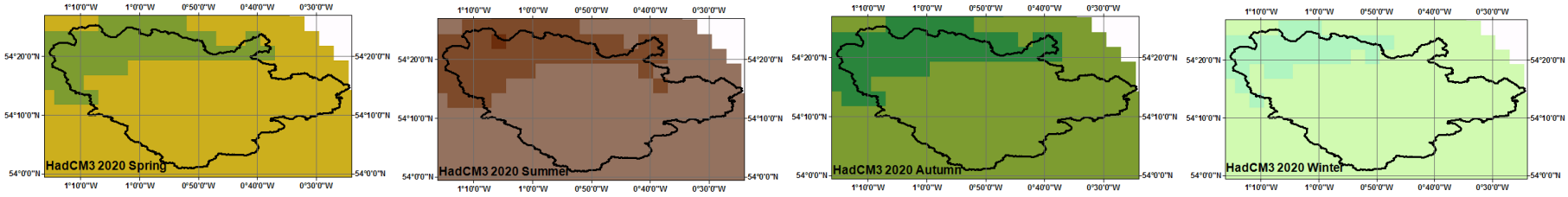
HadCM3 2020 Spring
HadCM3 2020 Summer
HadCM3 2020 Autumn
HadCM3 2020 Winter

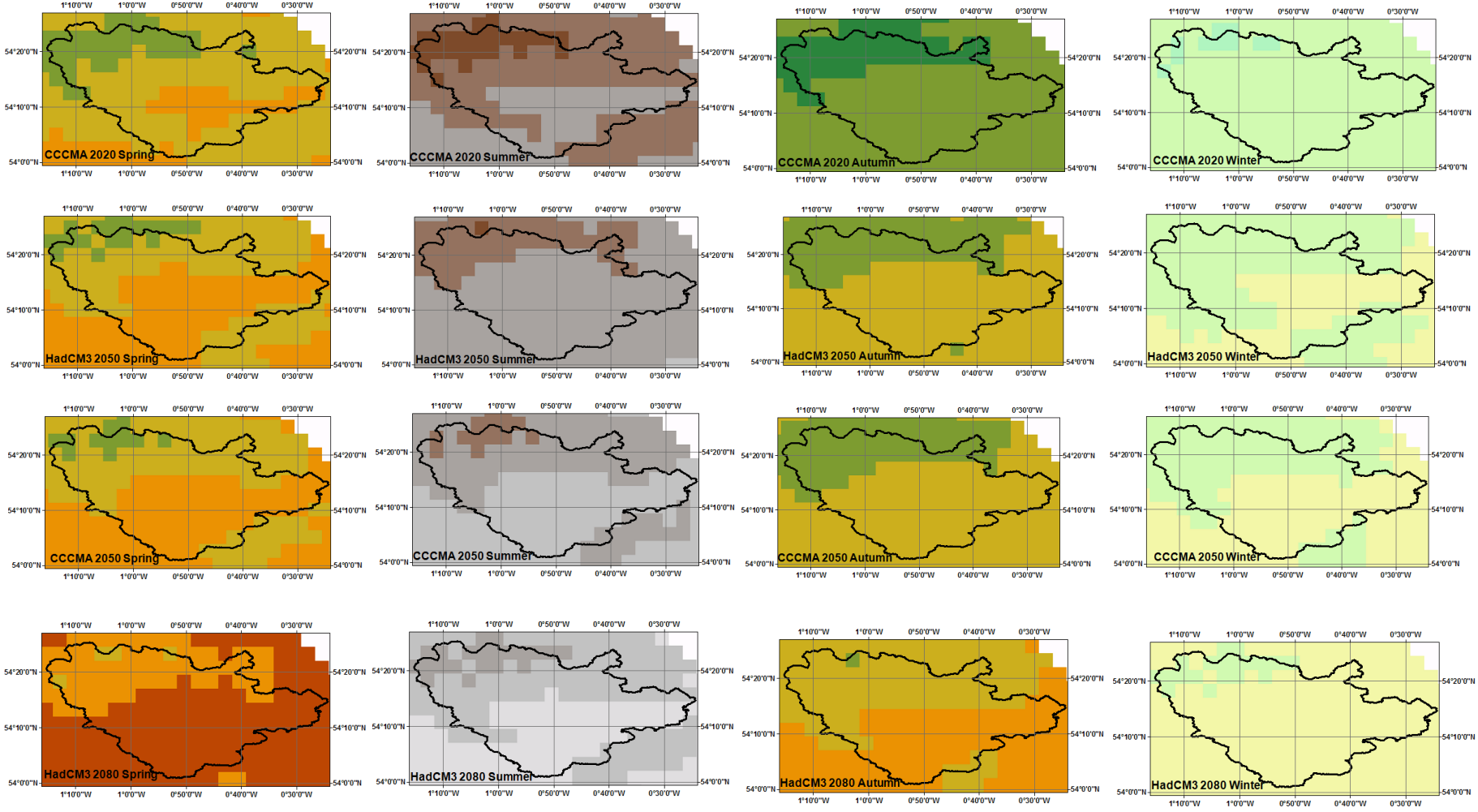
CCCMA 2020 Spring
CCCMA 2020 Summer
CCCMA 2020 Autumn
CCCMA 2020 Winter
HadCM3 2050 Spring
HadCM3 2050 Summer
HadCM3 2050 Autumn
HadCM3 2050 Winter
CCCMA 2050 Spring
CCCMA 2050 Summer
CCCMA 2050 Autumn
CCCMA 2050 Winter
HadCM3 2080 Spring
HadCM3 2080 Summer
HadCM3 2080 Autumn
HadCM3 2080 Winter

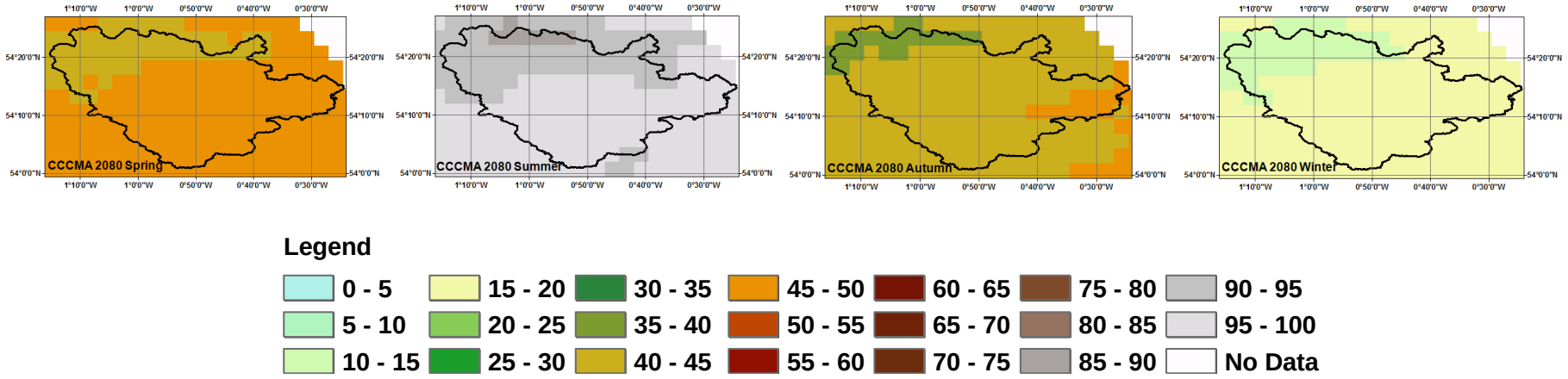

Figure 4 The comparison of changes in seasonal monthly mean PET (estimated using Blaney-Criddle method) as obtained from CCCMA and HadCM3 Models (bias uncorrected) on the River Dewent catchment, Yorkshire-Humberside for study instants like 2020, 2050 and 2080 ((a): In the upper row the four maps show the average values of temperature (in ^{0}C) in seasons like spring, summer, autumn and winter as obtained from HadCM3 for the study instants 2020; (b): maps from CCCMA for the study instants 2020; (c): maps from HadCM3 for the study instants 2050; (d): maps from CCCMA for the study instants 2050; (e): maps from HadCM3 for the year 2080; (f): maps from CCCMA for the study instants 2080)

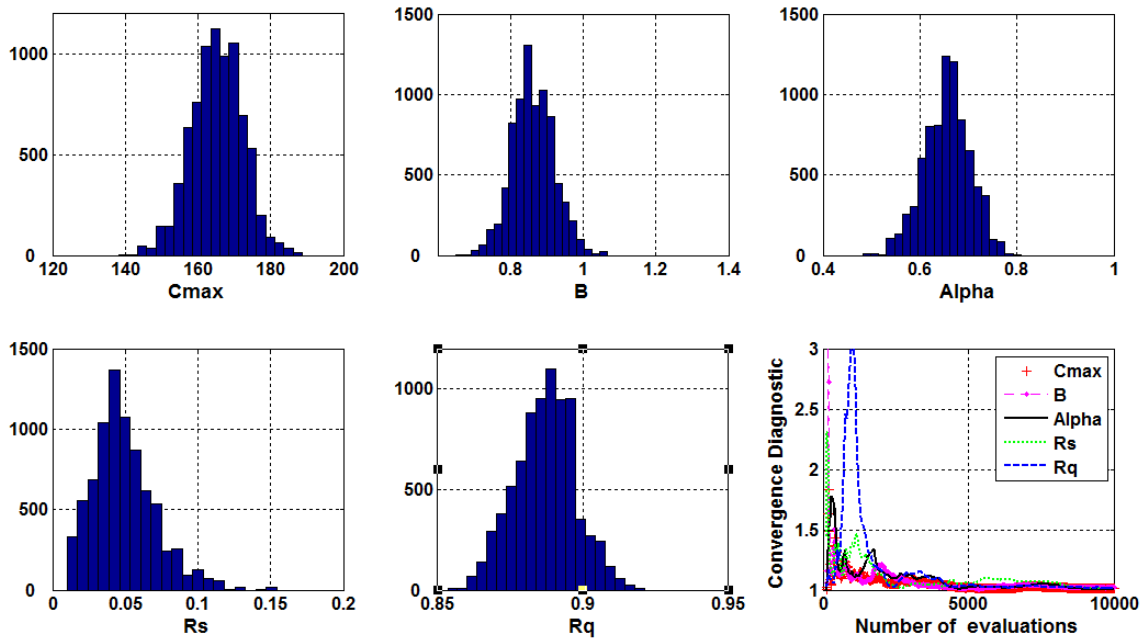

Figure 5: Display of distributions of the parameters and evolution of GR scale-reduction convergence diagnostic for the parameters in the auxiliary - HyMOD model using monthly runoff data from the River Derwent catchment and SCEM-UA (2(a) to 2(d) corresponds to parameters like Cmax, bexp, Alpha, Rs and Rq; 2(e) corresponds to variation of GR convergence diagnostic for these parameters)

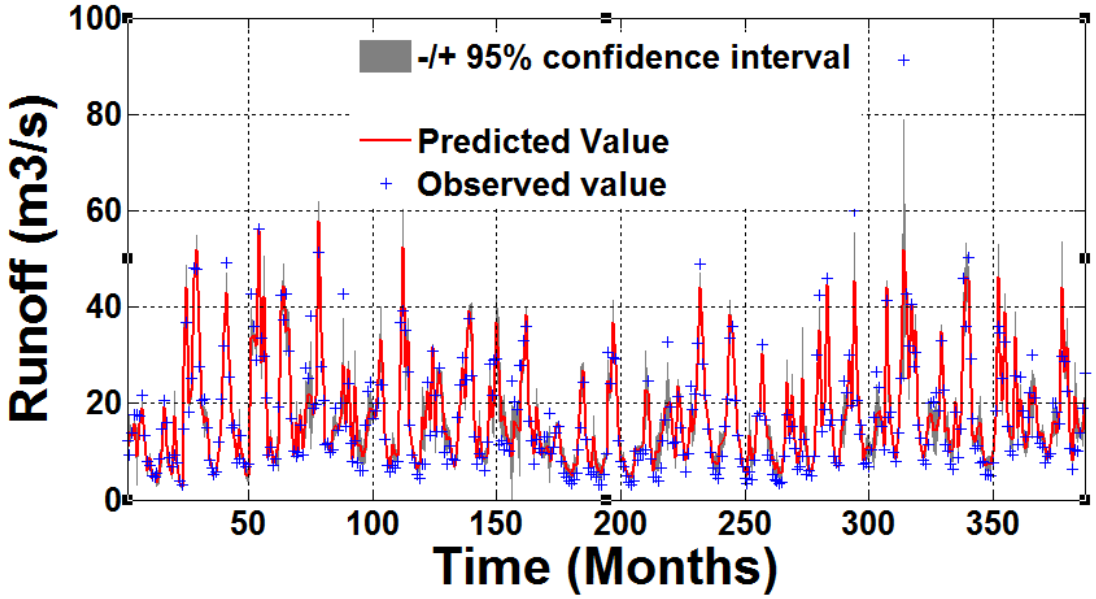

Figure 6: Runoff forecasting by SCEM-UA parameter estimation of the auxiliary - HyMOD for the River Derwent Catchment ((shaded area with 95% uncertainty bound)

1

2

3

4

5

6

7

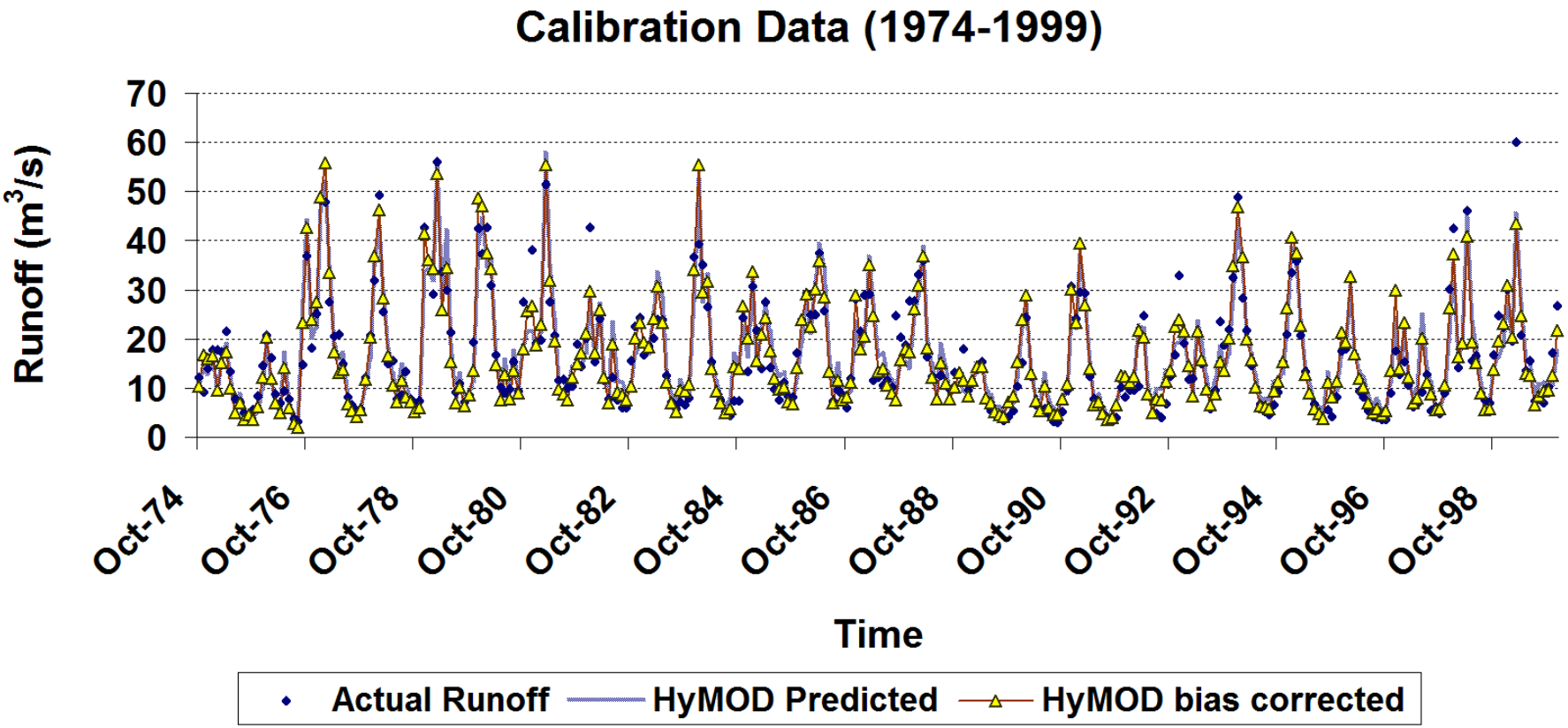

Figure 7: The scatter plot of performance of auxiliary-HyMOD under calibration data

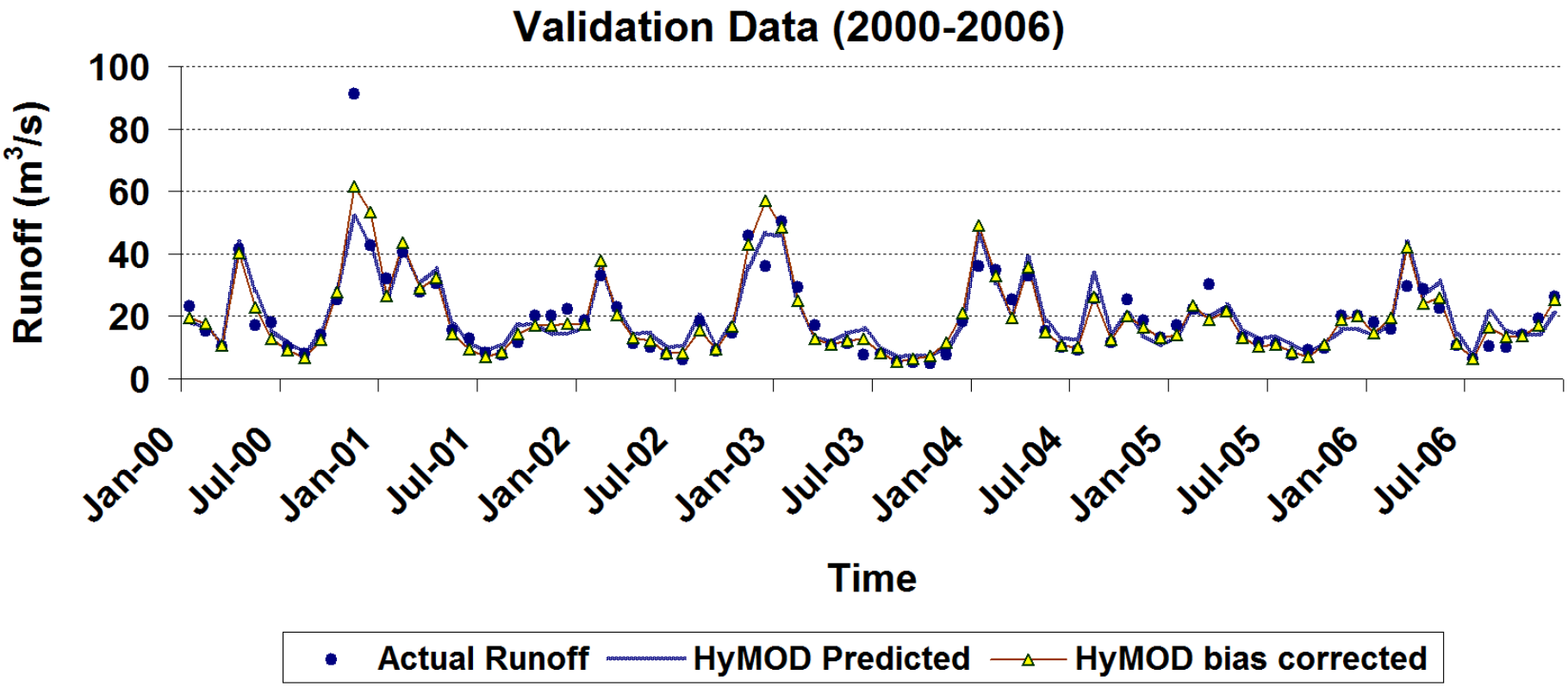

Figure 8: The scatter plot of performance of auxiliary-HyMOD under validation data

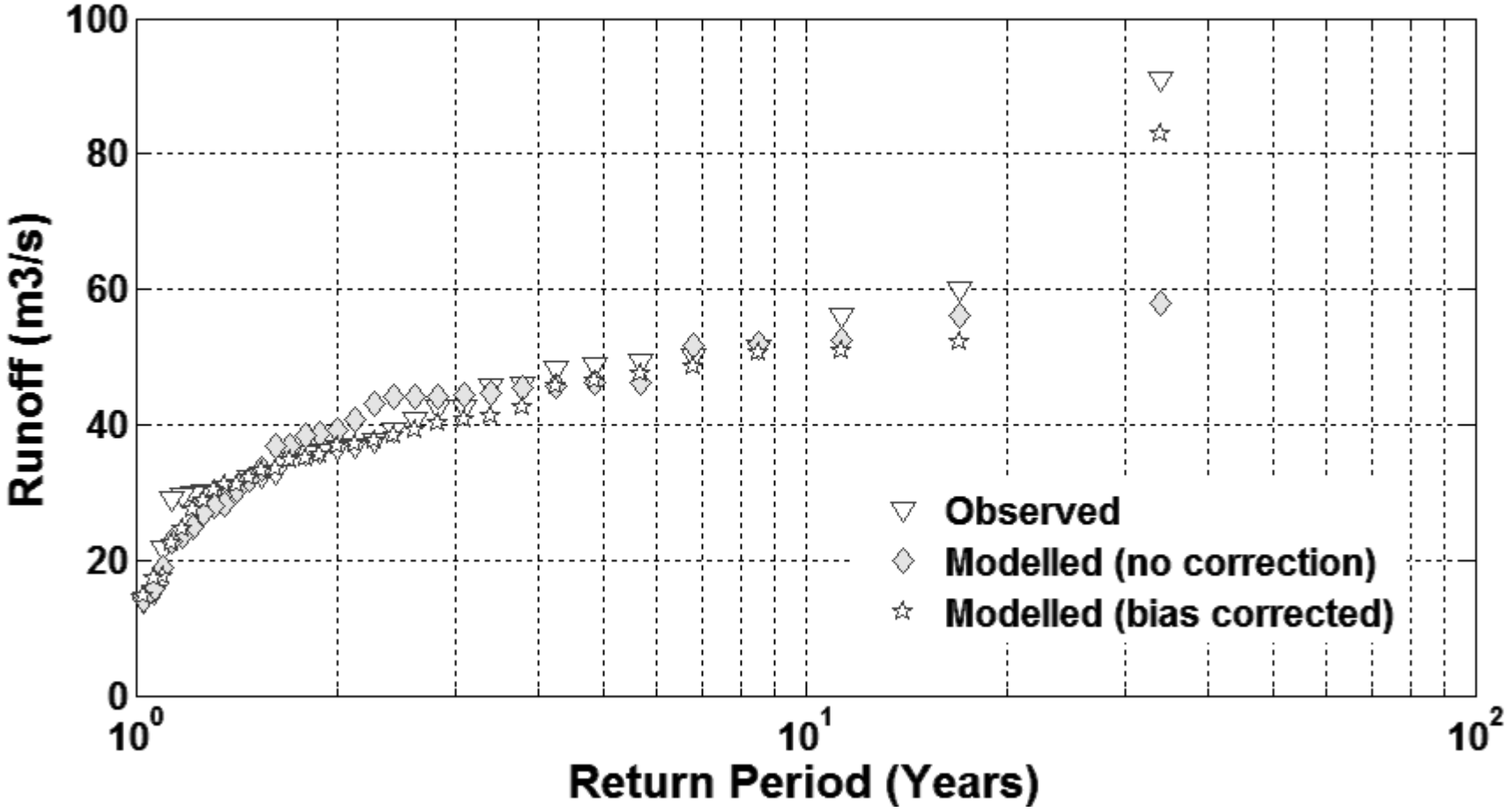
100
80
60
40
20
0
Runoff (m3/s)
10^0
10^1
10^2
Return Period (Years)
Observed
Modelled (no correction)
Modelled (bias corrected)

Figure 9: Flood frequency curves derived from observed, auxilary - HyMOD modelled and auxilary - HyMOD modelled (bias corrected) mean flow time series at the River Derwent, Yorkshire-Humberside

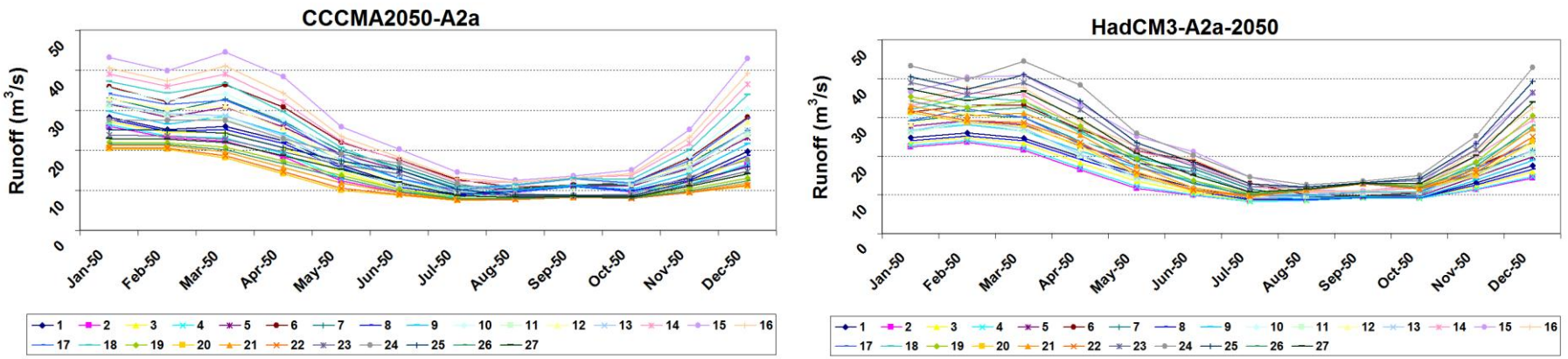

Figure 10: The hydrological simulation results from different ensemble combinations of GCM data in Derwent catchment during 2050s [a). CCCMA-A2a, b). HadCM3-A2a

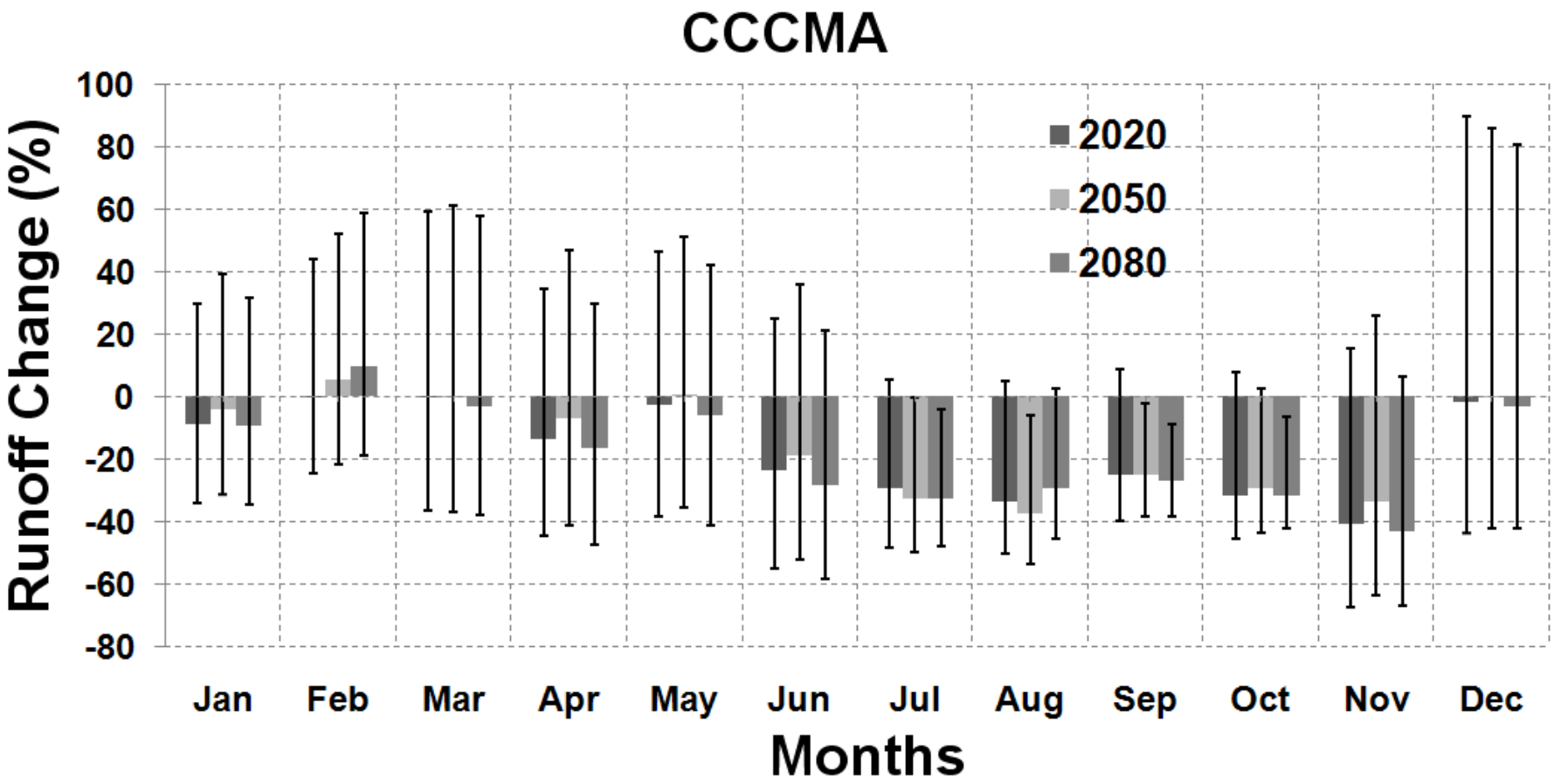

Figure 11: Percentage change in mean monthly streamflow between the observed 1999-2008 period and future scenarios for 2020, 2050 and 2080 time-slices using the SRES A2a CCCMA Model, at the River Derwent catchment, Yorkshire-Humberside

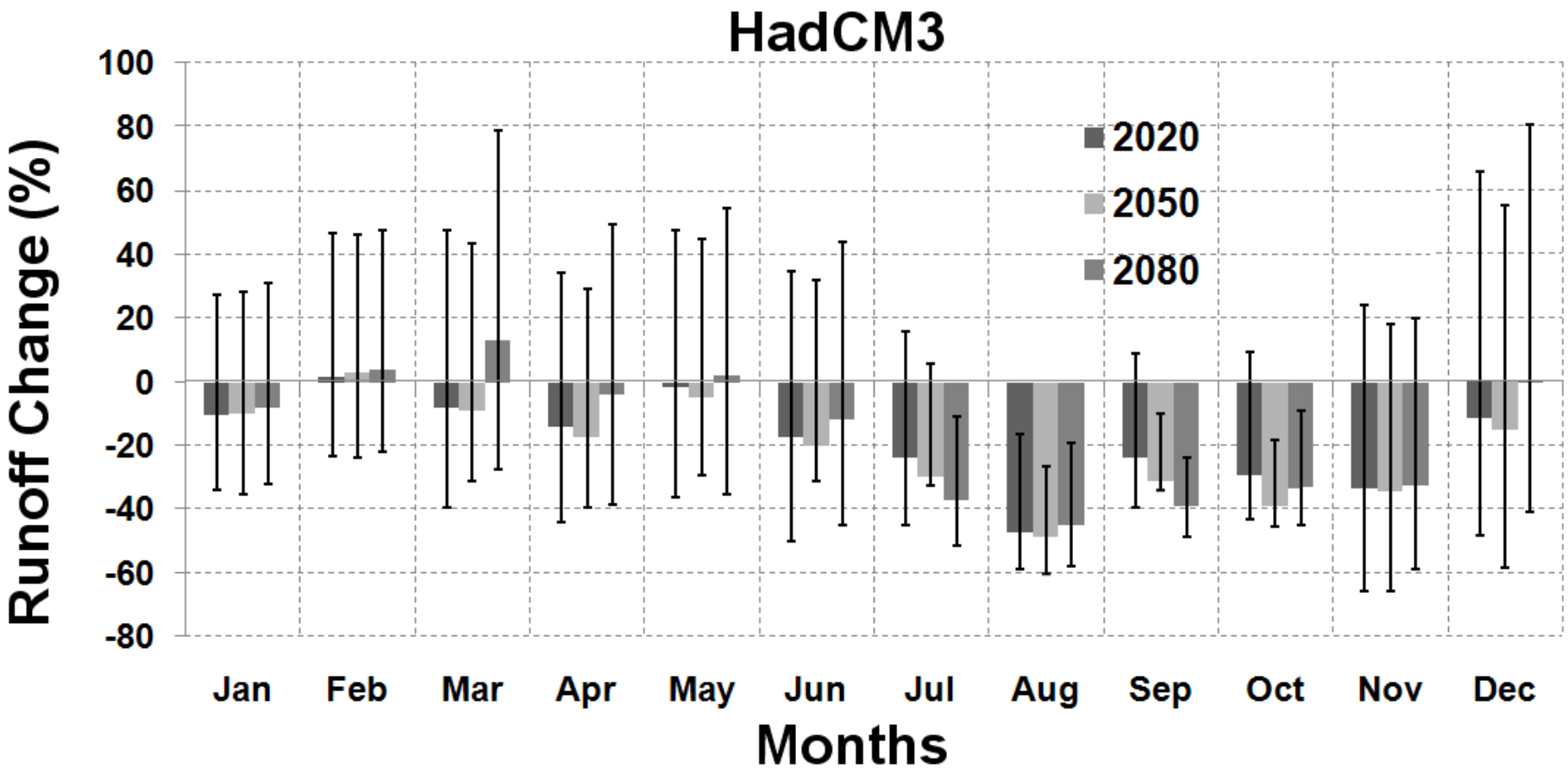
HadCM3
Runoff Change (%)
100
80
60
40
20
0
-20
-40
-60
-80
2020
2050
2080
Jan
Feb
Mar
Apr
May
Jun
Jul
Aug
Sep
Oct
Nov
Dec
Months

Figure 12: Percentage change in mean monthly streamflow between the observed 1999-2008 period and future scenarios for 2020, 2050 and 2080 time-slices using the SRES A2a HadCM3 Model, at the River Derwent catchment, Yorkshire-Humberside

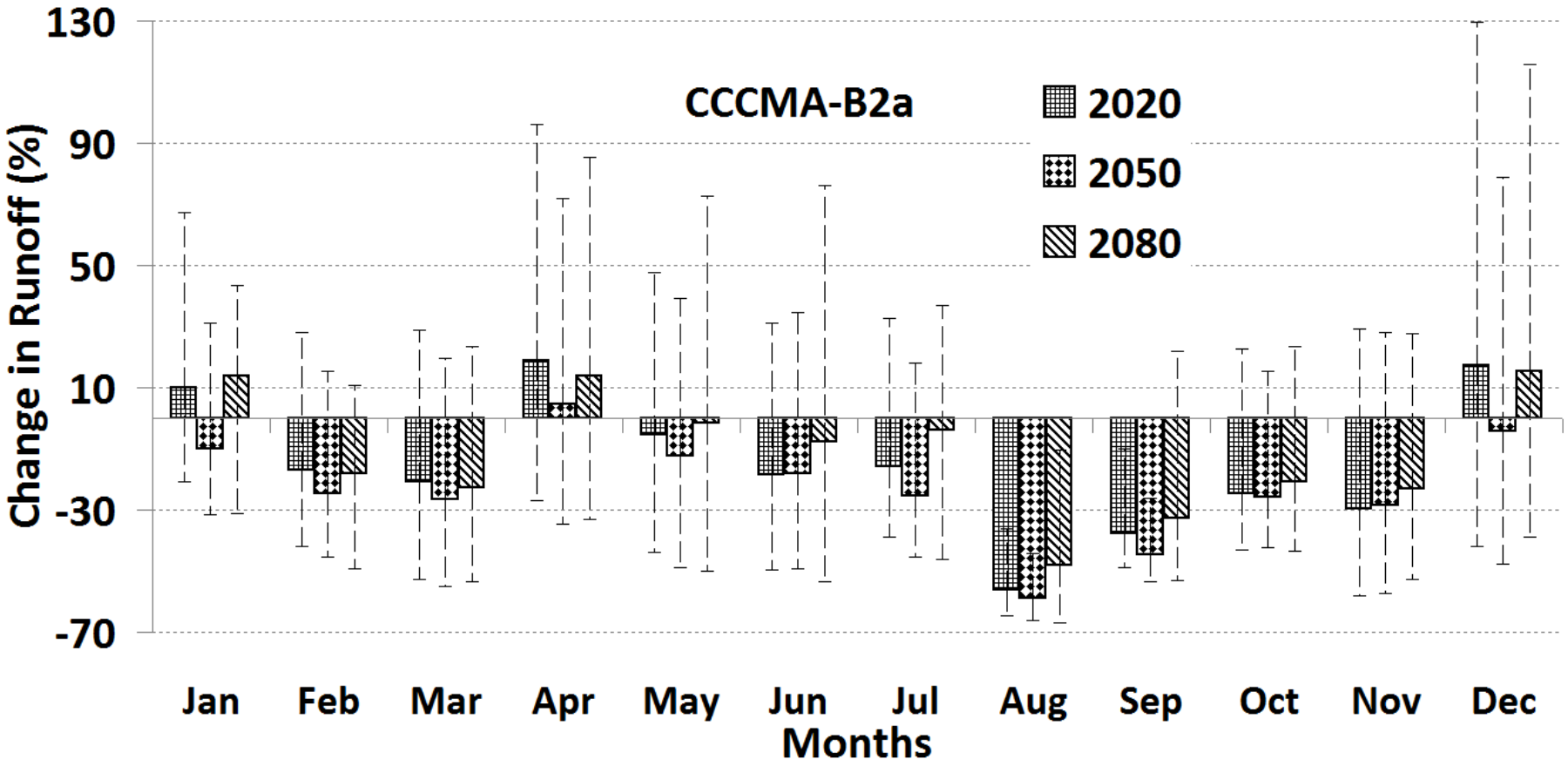

Figure 13: Percentage change in mean monthly streamflow between the observed 1999-2008 period and future scenarios for 2020, 2050 and 2080 time-slices using the SRES B2a CCCMA Model, at the River Derwent catchment, Yorkshire-Humberside

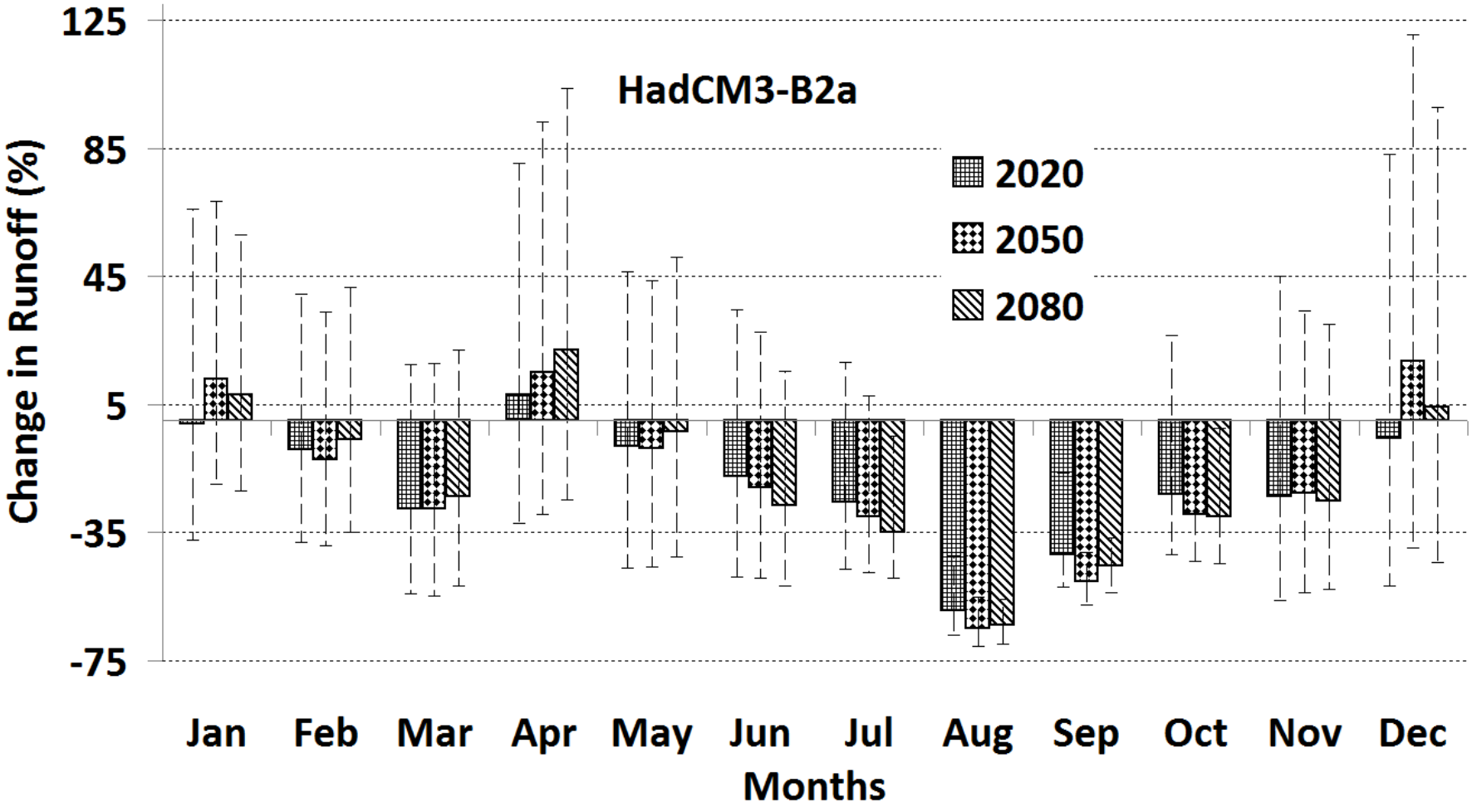
HadCM3-B2a
2020
2050
2080
Change in Runoff (%)
125
85
45
5
-35
-75
Jan
Feb
Mar
Apr
May
Jun
Jul
Aug
Sep
Oct
Nov
Dec
Months

Figure 14: Percentage change in mean monthly streamflow between the observed 1999-2008 period and future scenarios for 2020, 2050 and 2080 time-slices using the SRES A2a HadCM3 Model, at the River Derwent catchment, Yorkshire-Humberside

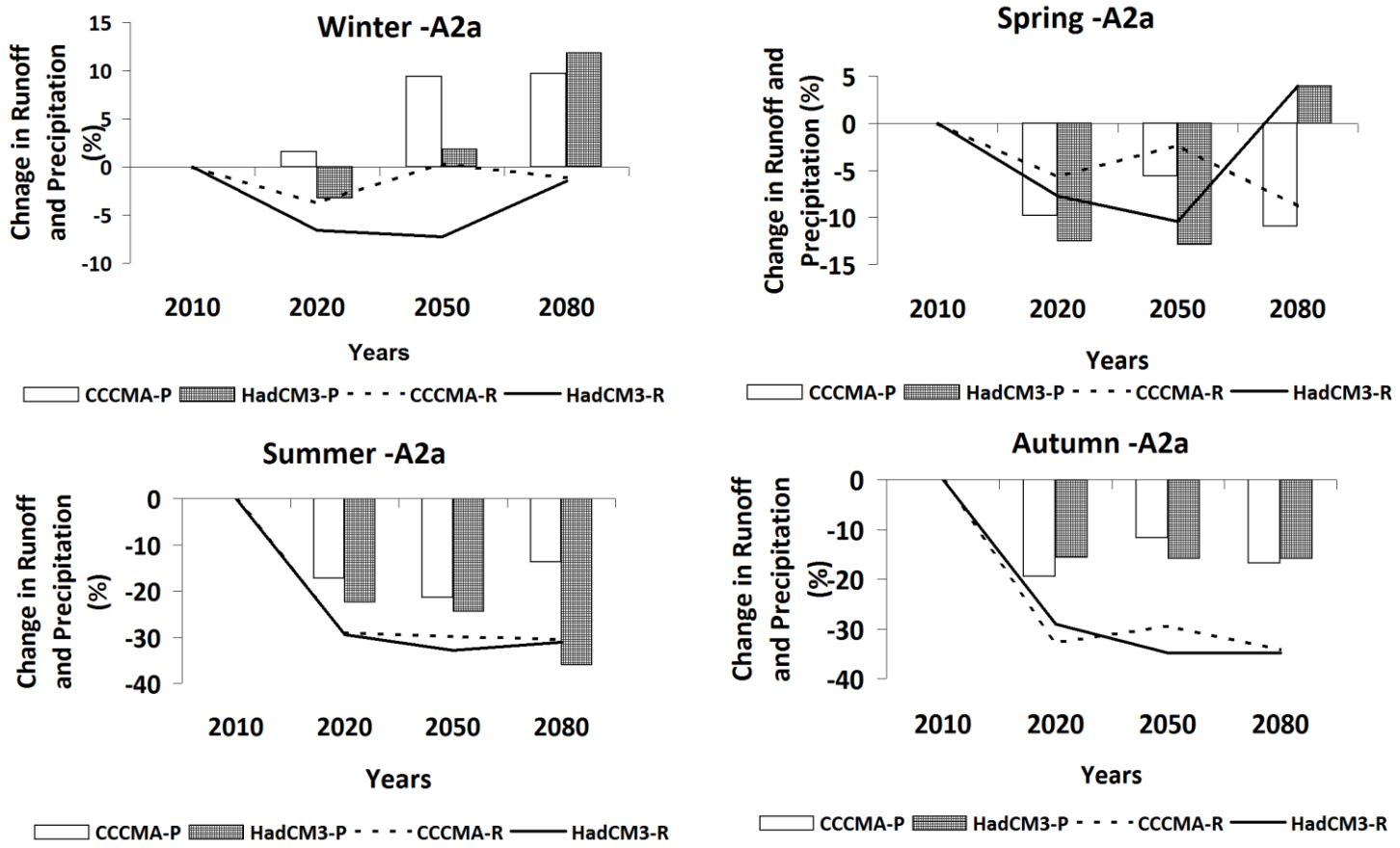

Figure 15: Simulated percentage change in effective runoff in different seasons for each future time period considered (2020s, 2050s and 2080s) using SRES A2a CCCMA and HadCM3 forcing data , along with corresponding change in mean precipitation [(a) winter, (b) spring, (c) summer, (d) autumn] (NB: P corresponding to precipitation data and R corresponding to runoff data)

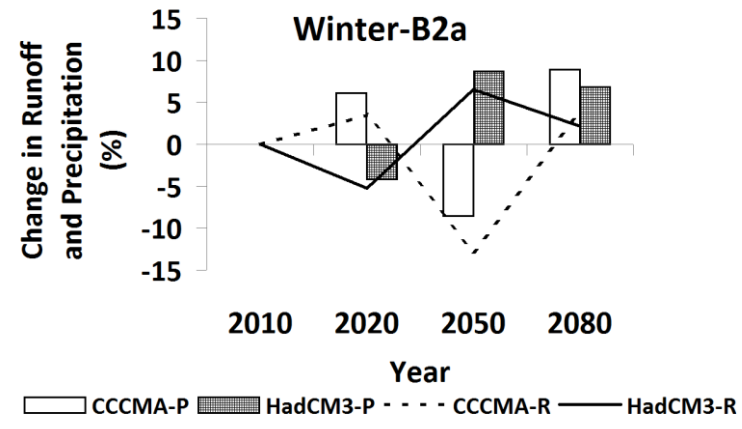
Winter-B2a
Change in Runoff and Precipitation (%)
15
10
5
0
-5
-10
-15
2010
2020
2050
2080
Year
CCCMA-P
HadCM3-P
CCCMA-R
HadCM3-R

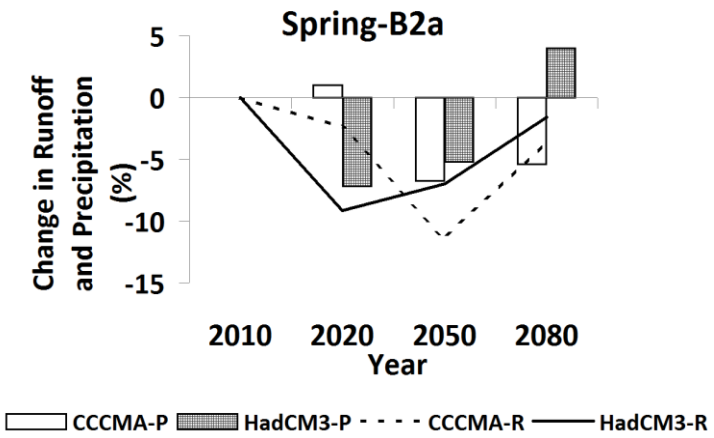
Spring-B2a
Change in Runoff and Precipitation (%)
5
0
-5
-10
-15
2010
2020
2050
2080
Year
CCCMA-P
HadCM3-P
CCCMA-R
HadCM3-R

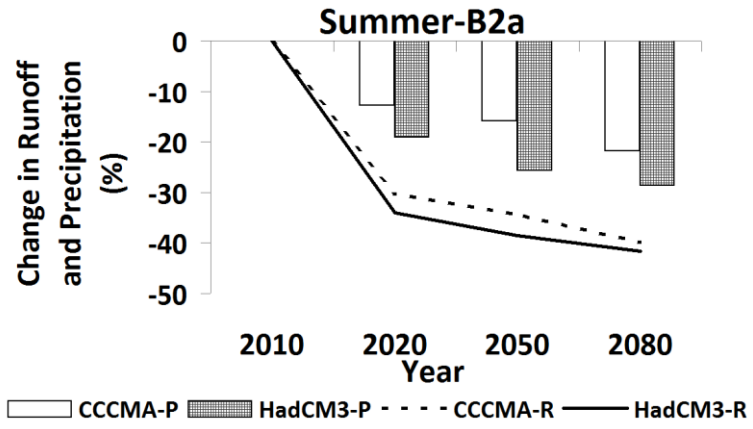
Summer-B2a
Change in Runoff and Precipitation (%)
0
-10
-20
-30
-40
-50
2010
2020
2050
2080
Year
CCCMA-P
HadCM3-P
CCCMA-R
HadCM3-R

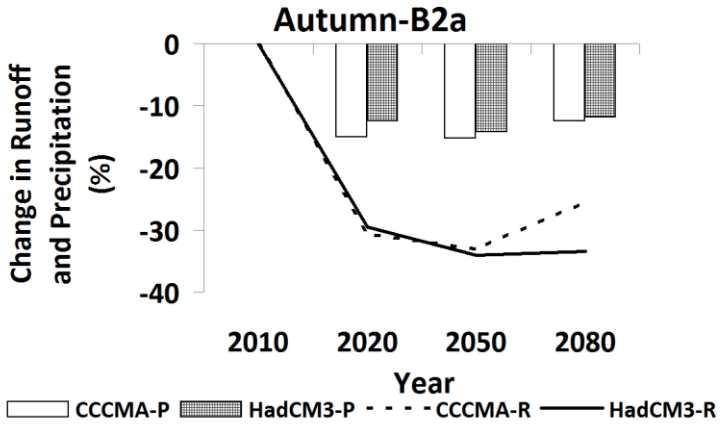
Autumn-B2a
Change in Runoff and Precipitation (%)
0
-10
-20
-30
-40
2010
2020
2050
2080
Year
CCCMA-P
HadCM3-P
CCCMA-R
HadCM3-R

Figure 16: Simulated percentage change in effective runoff in different seasons for each future time period considered (2020s, 2050s and 2080s) using SRES A2a CCCMA and HadCM3 forcing data , along with corresponding change in mean precipitation [(a) winter, (b) spring, (c) summer, (d) autumn] (NB: P corresponding to precipitation data and R corresponding to runoff data)

Table 1: Comparison of decadal trends of average precipitation and temperature in the Brue catchment with corresponding values in the antecedent decade.

Decades	1914-1919	1920-1929	1930-1939	1940-1949	1950-1959	1960-1969	1970-1979	1980-1989	1990-1999	2000-2006	1914-1919 and 2000-2006
Average Precipitation											
Winter	-	-11.94	7.30	-11.22	4.51	-9.23	7.62	-13.59	13.46	-1.78	-17.52
spring	-	-0.23	15.87	-17.55	2.72	8.79	-0.55	14.57	-21.39	30.27	24.27
summer	-	2.66	-9.85	1.22	15.98	-16.20	-13.04	13.93	-13.39	31.16	2.45
autumn	-	3.21	21.94	-15.81	0.31	6.32	-17.16	7.37	-0.84	25.20	24.79
Average Temperature											
Winter	-	11.34	0.59	-18.34	-1.66	-14.07	31.37	-5.47	22.36	8.99	27.99
spring	-	2.81	0.82	6.14	-5.78	-1.42	-3.62	2.24	13.41	1.50	15.91

summer	-	-1.07	5.89	-0.69	-2.71	-2.44	2.32	0.30	4.11	3.49	9.17
autumn	-	3.10	4.94	3.58	-3.22	-0.61	-1.22	2.62	0.95	9.76	21.06

Table 2: Percentage comparison of different seasonal meteorological variables obtained from different GCMs under different scenarios with corresponding values obtained during 2000-2006 period.

	Mean Precipitation			**Mean Temperature**			**Mean PET**		
				CCCMA-A2a					
	2020s	***2050s***	***2080s***	***2020s***	***2050s***	***2080s***	***2020s***	***2050s***	***2080s***
winter	1.59	9.36	9.69	2.39	26.7	38.15	1.91	20.59	31.35
spring	-9.81	-5.59	-10.91	4.04	9.39	15.8	3.31	7.82	13.64
summer	-17.25	-21.44	-13.67	-0.15	7.95	15.25	-0.06	7.57	14.45
autumn	-19.45	-11.68	-16.74	-2.62	10.46	16.76	-2.45	8.92	14.67
				CCCMA-B2a					
winter	6.12	-8.57	8.92	13.55	3.42	18.98	11.53	2.72	15.74

spring	0.99	-6.74	-5.4	2.55	7.68	12.18	1.72	6.51	10.42
summer	-12.75	-15.86	-21.83	1.08	3.63	8.72	1.1	3.47	8.28
autumn	-15.06	-15.23	-12.48	0.09	4.36	12.54	-0.06	3.52	11.04
				HadCM3-A2a					
winter	-3.25	1.85	11.85	-8.6	22.29	45.94	-6.16	17.71	38.59
spring	-12.52	-12.9	3.96	2.22	8.85	26.55	2	7.73	23.15
summer	-22.37	-24.36	-35.96	-2.48	4.77	13.15	-2.29	4.57	12.45
autumn	-15.56	-15.83	-15.81	-2.95	9.65	21.05	-2.55	8.75	18.68
				HadCM3-B2a					
winter	-4.15	8.67	6.8	-1.21	10.78	23.91	0.08	7.71	20.23
spring	-7.16	-5.19	4.01	1.69	7.88	16.59	1.49	7.19	14.82
summer	-19.09	-25.68	-28.66	-1.68	3.07	8.07	-1.58	2.95	7.7
autumn	-12.47	-14.22	-11.84	2.54	4.32	12.03	2.05	3.21	10.27

Footnote: The units are in %

Table 3: Prior uncertainty associated with parameters and their expected values in auxiliary – HyMOD model applied to River Derwent Catchment

Parameters	**Description**	**Monthly Data**

		Units	Lower bound	Upper bound	Behaviour range	Expected value
Cmax	Maximum storage capacity in catchment	mm	10	800	162.82 – 168.43	165.746
bexp	Factor distributing flow between two series of reservoirs	-	0.01	2	0.847 – 0.883	0.8657
Alpha	Shape factor for the main soil water storage tank	-	0.01	2	0.659 – 0.683	0.6657
Rs	Residence time of linear slow flow reservoirs	month	0.01	2	0.034 – 0.046	0.0367
Rq	Residence time of linear quick flow reservoirs	month	0.01	2	0.884 – 0.892	0.8911

Table 4 The statistical indices for 33-years (Oct 1973- Dec 2006) continuous simulation of monthly discharges at the River Derwent catchment at Yorkshire-Humberside (before and after model bias correction).

1

Months →		Jan	Feb	Mar	Apr	May	Jun	Jul	Aug	Sep	Oct	Nov	Dec	Annual
Conditions and Parameters ↓														
No Bias Correction	Bias	0.760	1.03	-1.834	-2.05	-3.5	-2.82	-2.106	-2.59	-2.03	-0.26	3.71	4.090	-0.638
	MAE	3.976	3.66	4.532	3.231	4.14	3.31	2.201	2.867	3.44	2.91	4.53	5.647	1.346
	MSE	27.85	21.07	35.637	19.904	26.20	22.25	7.475	13.62	25.69	12.55	65.39	47.770	2.438
	RMSE	5.278	4.5906	5.969	4.46	5.118	4.71	2.734	3.69	5.06	3.54	8.08	6.911	1.561
	NS Efficiency	0.785	0.811	0.767	0.807	0.244	0.473	0.487	0.415	0.794	0.810	0.716	0.442	0.825
	CORR	0.902	0.909	0.896	0.926	0.914	0.626	0.826	0.901	0.549	0.902	0.956	0.812	0.945
After Bias Correction	Bias	-0.029	0.031	0.015	0.087	-0.019	-0.057	-0.036	-0.096	-0.098	-0.160	-0.281	-0.161	-0.299
	MAE	2.827	2.686	3.844	2.396	1.23	1.255	0.703	1.074	2.019	1.978	2.9028	3.091	1.344
	MSE	16.353	11.68	28.422	10.66	2.708	2.214	0.814	2.221	12.18	6.381	13.16	16.47	2.384

	RMSE	4.043	3.417	5.331	3.265	1.645	1.488	0.902	1.49	3.490	2.526	3.628	4.058	1.544
	NS Efficiency	0.874	0.895	0.814	0.897	0.921	0.85	0.870	0.904	0.882	0.903	0.943	0.807	0.849
	CORR	0.935	0.946	0.902	0.947	0.960	0.924	0.934	0.952	0.701	0.951	0.971	0.900	0.951

Table 5: Statistical indices used to compare training and testing phase of auxiliary- HyMOD

	Training Data	Validation Data
CORR	0.87	0.83
Slope	0.94	0.85
Intercept	1.4	3.08

Table 6: Different combinations of inputs used for hydrological simulation

Ensemble number	Member details
1	Mean P and catchment spatial Mean of PETmean (calculated from GCM mean temperature data)
2	Mean P and catchment spatial maximum value from PETmax (calculated from GCM maximum temperature data)
3	Mean P and catchment spatial minimum value from PETmax(calculated from GCM maximum temperature data)
4	Mean P and catchment spatial Mean Value from PETmax (calculated from GCM maximum temperature data)
5	Mean P and catchment spatial Maximum value from PETmin (calculated from GCM minimum temperature data)
6	Mean P and catchment spatial Minimum Value from PETmin (calculated from GCM minimum temperature data)
7	Mean P and catchment spatial mean value from PETmin (calculated from GCM minimum temperature data)
8	Mean P and catchment spatial Maxmimum from PETmean (calculated from GCM mean temperature data)
9	Mean P and catchment spatial Minimum from PETmean (calculated from GCM mean temperature data)

10	Max P and catchment spatial Mean of PETmean (calculated from GCM mean temperature data)
11	Max P and catchment spatial maximum value from PETmax (calculated from GCM maximum temperature data)
12	Max P and catchment spatial minimum value from PETmax (calculated from GCM maximum temperature data)
13	Max P and catchment spatial Mean Value from PETmax (calculated from GCM maximum temperature data)
14	Max P and catchment spatial Maximum value from PETmin (calculated from GCM minimum temperature data)
15	Max P and catchment spatial Minimum Value from PETmin (calculated from GCM minimum temperature data)
16	Max P and catchment spatial mean value from PETmin (calculated from GCM minimum temperature data)
17	Max P and catchment spatial Maxmimum from PETmean (calculated from GCM mean temperature data)
18	Max P and catchment spatial Minimum from PETmean (calculated from GCM mean temperature data)
19	Min P and catchment spatial Mean of PETmean (calculated from GCM mean temperature data)
20	Min P and catchment spatial maximum value from PETmax (calculated from GCM maximum temperature data)
21	Min P and catchment spatial minimum value from PETmax (calculated from GCM maximum temperature data)
22	Min P and catchment spatial Mean Value from PETmax (calculated from GCM maximum temperature data)
23	Min P and catchment spatial Maximum value from PETmin (calculated from GCM minimum temperature data)

24	Min P and catchment spatial Minimum Value from PETmin (calculated from GCM minimum temperature data)
25	Min P and catchment spatial mean value from PET min (calculated from GCM minimum temperature data)
26	Min P and catchment spatial Maxmimum from PETmean (calculated from GCM mean temperature data)
27	Min P and catchment spatial Minimum from PETmean (calculated from GCM mean temperature data)

Footnote: The notations like P, PETmean, PETmean and PETmin are corresponding to time series like precipitation, maximum potential evapotranspiration, mean potential evapotranspiration and minimum potential evapotranspiration respectively.

Table 7: The annual average runoff calculated using data from different Climate Models under Scenarios and corresponding months with maximum and minimum runoff

Periods	**Baseline Period**			**Annual runoff calculated using data from different Climate Models under Scenarios and months with maximum and minimum runoff**											
				HadCM3						**CCCMA**					
				A2a			**B2a**			**A2a**			**B2a**		
	Min	**Ave**	**Max**	**Min**	**Ave**	**Max**	**Min**	**Ave**	**Max**	**Min**	**Ave**	**Max**	**Min**	**Ave**	**Max**
1999-2008	222.08 (Jul)	395.62	624.57 (Jan)	-	-	-	-	-	-	-	-	-	-	-	
2020s	-	-	-	130.39 (Aug)	332.09	560.74 (Jan)	100.54 (Aug)	332.78	617.56 (Jan)	156.41 (Jul)	335.15	567.40 (Jan)	108.90 (Aug)	353.03	688.14 (Jan)

2050s	-	-	-	126.52 (Aug)	322.47	561.78 (Jan)	86.83 (Aug)	346.76	705.61 (Jan)	149.16 (Jul)	347.83	597.31 (Jan)	101.64 (Aug)	316.53	562.90 (Jan)
2080s	-	-	-	136.75 (Jul)	349.46	596.49 (Mar)	89.26 (Aug)	344.02	676.02 (Jan)	149.0 (Jul)	333.1	579.09 (Feb)	128.30 (Aug)	362.63	710.35 (Jan)